Spatiotemporal Analysis and Modeling of Urban Growth Using SLEUTH Model: A Case of Assosa City

Seid Muhammed Ahmed

A Thesis Submitted to Department of Geomatics Engineering

School of Civil Engineering and Architecture

Presented in Partial Fulfillment of the Requirement for the Degree of Master's in Geoinformatics

Office of Graduate Studies

Adama Science and Technology University

September, 2022

Adama, Ethiopia

Spatiotemporal Analysis and Modeling of Urban Growth Using SLEUTH Model: A Case of Assosa City

Seid Muhammed Ahmed

Advisor: Dejene Tesema Bulti (PhD)

A Thesis Submitted to Department of Geomatics Engineering
School of Civil Engineering and Architecture

Presented in Partial Fulfillment of the Requirement for the Degree of Master's in Geoinformatics

Office of Graduate Studies
Adama Science and Technology University

September, 2022
Adama, Ethiopia

Declaration

I hereby declare that this Master Thesis entitled "Spatiotemporal Analysis and Modeling of Urban Growth Using SLEUTH Model: A Case of Assosa City" is my original work. That is, it has not been submitted for the award of any academic degree, diploma or certificate in any other university. All sources of materials that are used for this thesis have been duly acknowledged through citation.

Seid Muhammed Ahmed	________________	___________________.
Name of student	signature	date

Recommendation

I, the advisor of this thesis, hereby certify that I have read the revised version of the thesis entitled "Spatiotemporal Analysis and Modeling of Urban Growth Using SLEUTH Model: A Case of Assosa City" prepared under my guidance by Seid Muhammed Ahmed submitted in partial fulfillment of the requirements for the degree of Mater's of Science in Geoinformatics. Therefore, I recommend the submission of revised version of the thesis to the department following the applicable procedures.

Dejene Tesema Bulti (PhD)	______________.	_______________.
Major Advisor	Signature	Date

Approval sheet

I, the advisor of this thesis entitled, "Spatiotemporal Analysis and Modeling of Urban Growth Using SLEUTH Model: A Case of Assosa City" and developed by Seid Muhammed Ahmed, hereby certify that the recommendation and suggestions made by the board of examiners are appropriately incorporated into the final version of the thesis.

Dejene Tesema Bulti (PhD)	____________	____________.
Major Advisor	Signature	Date

We, the undersigned, members of the Board of Examiners of the thesis by Seid Muhammed Ahmed have read and evaluated the thesis entitled "Spatiotemporal Analysis and Modeling of Urban Growth Using SLEUTH Model: A Case of Assosa City" and examined the candidate during open defense. This is, therefore, to certify that the thesis is accepted for partial fulfillment of the requirement of the degree of Master of Science in Geoinformatics.

____________	____________	____________.
Chairperson	Signature	Date
____________	____________	____________.
Internal Examiner	Signature	Date
____________	____________	____________.
External Examiner	Signature	Date

Finally, approval and acceptance of the thesis is contingent upon submission of its final copy to the Office of Postgraduate Studies (OPGS) through the Department Graduate Council (DGC) and School Graduate Committee (SGC).

____________	____________	____________.
Department Head	Signature	Date
____________	____________	____________.
School Dean	Signature	Date
____________	____________	____________.
Office of Postgraduate Studies, Dean	Signature	Date

ACKNOWLEDGMENT

First of all, I would like to thank the "Almighty ALLAH", who helped me to accomplish my thesis. A special thanks to my advisor, Dr. Dejene Tesema for being generous in sharing knowledge for this study; for the guidance, support, and encouragement throughout; for devotedly contributing towards the success of this study. Your words of inspiration and confidence in me will never be forgotten.

I am grateful to acknowledge Assosa University for granting me the chance to pursue my studies at Adama Science and Technology University. I also want to thank those seniors who paved the way to my journey in my academic career. Last but not least I appreciate those people around me with the courage to date that has a profound positive impact on my academic journey.

TABLE OF CONTENTS

LIST OF TABLE

LIST OF FIGURE

LIST OF ACRONYMS

ASTER	Advanced Space borne Thermal Emission and Reflection Radiometer
CA	Cellular Automata
DEM	Digital Elevation Model
ENVI	Environment for Visualizing Images
ETM+	Enhanced Thematic Mapper Plus
GCP	Ground Control Point
GIS	Geographic Information System
GIF	Graphics Interchange Format
GPS	Global Positioning System
LULC	Land Use Land Cover
SLUETH	Slope Land use Urbanization Exclusion Transportation Hill shade
SVM	Support vector machine
OLI	Operational Land Imager
TM	Thematic Mapper
UN	United Nations
USGS	United State Geological Survey
RS	Remote Sensing

ABSTRACT

Urbanization is a global trend with significant environmental effects, urging a clear policy at all levels. Analyzing the dynamics of urban growth on both spatial and temporal scales, as well as future potential growth, has been recognized as a critical step in understanding the consequences of urbanization and developing long-term planning strategies. In this study, Asossa City, one of the rapidly growing regional cities in Ethiopia, is considered to analyze its spatiotemporal growth from 1990 to 2021 and to predict its potential future expansion in the years 2030, 2040, and 2050 under different growth scenarios. Through supervised image classification using the support vector machine algorithm, LULC maps of the study area in 1990, 2000, 2010, and 2021 were prepared, and the spatiotemporal changes of LULC were investigated. Five selected spatial metrics (number of patches, patch density, edge density, largest patch index, and area weighted mean patch fractal dimension) were used to examine the dynamics of landscape structure in the study area over time. Urban development typologies were also analyzed using the spatial link between pre-growth and newly built components. By modeling the growth of the study area using the SLEUTH model, the future potential growth extent of the city was forecasted for the years 2030, 2040, and 2050, under three growth scenarios: business as usual, planned growth, and environment-protecting. The results show that the built-up area has undergone about 14% expansion annually in the past 31 years, indicating rapid urban growth. The urban area of the city experienced a fragmented urban growth process, particularly, at the fringe, while the core of the city underwent relatively compact growth by infilling open spaces and through edge expansion over time. Moreover, the prediction results of business as usual scenario indicates that 1801.7ha, 2493.33ha and 3267.4ha of land will be covered by built-up area in 2030, 2040 and 2050 respectively. Similar to this, the predicted result of planed growth scenario indicates that the built up area will reach 1723.9ha, 2207.8ha and 2885.7ha in 2030, 2040 and 2050. In environment-protecting scenario Built-up area will be 1718 ha in 2030 and 2179.9ha in 2040. In 2050 it was predicted as 2778.6ha. This study would assist planners and prospective stakeholders in planning a new heading before adverse effects become unavoidable. The formulation of urban planning policy should also work to strike a balance between socioeconomic requirements and the sustainable use of finite resources.

Keywords: *Land Use Land Cover; Landscape Metrics; SVM; SLEUTH model; Urban Growth.*

CHAPTER ONE: INTRODUCTION

1.1 Background of the study

Urban growth is a significant economic and social phenomena occurring at an unmatched rate and scale worldwide. Urban growth models have been developed and extensively adopted to study urban expansion and its impact on the ambient environment (Xuecao Li, and Peng Gong, 2016). These models can be employed in urban policymaking or analyses of development scenarios. The dynamicity of urban expansion leads to basic changes resulting in different impacts on the landscape structure and functions, at a large range of scales (Dietzel C., Herold M, Hemphill JJ., & Clarke KC, 2005; Sun S., Parker DC, Huang Q, Filatova T., et al., 2014). Regionally, urban growth is based on the infrastructure establishments such as industries, factories, construction of roads etc., and service facilities like hotels, hospitals etc., becomes gateway for promoting urbanization (Sudhira HS, Ramachandra, TV, & Jagadish KS,2004). Considering the global scenario, developing countries, still in transition, are more populated than the developed countries where the transformation is complete since two or three decades (Ranbir and Chitra, 2019)

According to the world urbanization prospects reported by the United Nations (UN, 2012), from 1965 to 2010, the global population increased from 3.3 billion to 6.9 billion, and the total amount of population will exceed 9.3 billion by 2050. Along with the population growth, more and more people chose to live in urban areas. The percentage of the world's population residing in urban areas increased from 35.5% in 1965 to 51.6% in 2010, and, by 2050, this number will reach at 67.2% (UN, 2012), which means over half of the population on the earth will live in urban areas by 2050. The increasing urban population causes increasing demand on urban land use. This movement leads to tremendous rural-urban land conversion, which has become a significant research topic in recent decades (Angel et al., 2007; Bhatta et al., 2010b; Martinuzzi et al., 2007; Sudhira et al., 2004; Wu et al., 2015).

Unprecedented urbanization causes rapid urban expansion, which can be unhealthy without reasonable urban planning. Some researchers employ the term "urban sprawl" to describe unhealthy urban expansion (Angel et al., 2011; Jat et al., 2008). Unhealthy urban expansion, or in other words, urban sprawl, refers to an uncontrolled and dispersed process of urban growth characterized by low population density and low urban area density (Bhatta et al., 2010; Jiang et al., 2007), which has gained widespread social focus. In other words, urban sprawl is defined as low density residential and commercial development on undeveloped land. Most of the time, people will move from these areas to try to find better areas to live. Urban sprawl increases congestion, decreases the urban employment rate, and decreases access to public services.

It directly causes many environmental and social problems, such as traffic problems, loss of open space, uneven distribution of local resources, and increased crime (Bhatta et al., 2010, Ji et al., 2006; Jiang et al., 2007; Lambin et al., 2001; Sudhira et al., 2004; Yu & Ng, 2007).

The majority of urban growth due to human activities is currently proceeding more quickly in the developing countries than in the developed countries. As the largest developing country in the world, Ethiopia has one of the world's fastest-growing economies. According to the Central Intelligence Agency (2018), its Gross Domestic Products (GDP) grew by 8.0% in 2016/17, which is slightly lower than a growth rate of 10.4% in 2014. The economy is a mixed, diversifying, and transformational economy with a large public sector. Ethiopian economy produces goods and services to feed its citizens and some for export (Central Intelligence Agency, 2018). According to this report, Investments in the energy and transport infrastructure are new reforms to speed up industrialization, such as the development of industrial parks; and continued progression in services are expected to lead urban growth. Therefore it is essential to have a clear vision of sustainable urbanization patterns in order to be able to design policies with a significant impact towards sustainability. Such knowledge is necessary for the optimal use of space, services, facilities and energy, which will lead to maximizing the benefits of urban population while minimizing both economic and environmental cost.

Most cities in developing countries are expanding horizontally following the routes of roads and railway networks, the urban sprawl is moving to unsettled peripheries at the expense of agricultural lands and areas of natural beauty and other surrounding ecosystems (Bekalo, 2009; Shiferaw and Tesfaw, 2017). Such dynamism in urban land cover can be caused by demographic, economic, or industrial factors. Currently, these are the major environmental concerns that have to be analyzed and monitored carefully for effective land use management and planning. Furthermore, the rapid urban growth and the associated urban land cover changes attracted many researchers to study and monitor the changes (Bekalo, 2009). There is no information on the extent and patterns of changes that occurred in Assosa city over time. Besides, there are no extensive studies conducted related to urban growth and its impacts. Urban planners and decision-makers should consider the potential of geospatial tools to detect, monitor, and evaluate urban dynamics. The urban area in Assosa has increased rapidly over the past few decades (Assosa city municipality), therefore it seems necessary to analyses the trend of urban growth and deduce its future effects on other land cover features.

Taking advantages of modern measuring and mapping technologies at spatial scales with free and open source technology and large data availability can be easily met with appropriate understanding and usage of spatial data management and modeling systems. The need of urban models to translate historic growth into future prediction has been attempted successfully by various researchers worldwide. Based on the theoretical concepts laid by Von Neumann and Ulam, Mathematicians like Conway developed ‘‘game of life’’ (Gardner Gardner, M., 1970) and Wolfram Wolfram, S., 1986) started to develop algorithms, studied rules of one-dimensional Cellular Automata (CA) having diverse applications. CA models can be defined as a class of two dimensional lattices of cells, where each cell representing a land use category tend to change its state over time depending on the local neighborhood of every cell. SLEUTH, a CA based model takes into account both spatiotemporal aspects of urban growth trajectories for simulation and prediction. The model is developed by Clarke, using terrain mapping and land cover deltatron. The acronym of SLEUTH stands for slope, land use, excluded, urban, transportation and hillshade, the layers used as input for the model, consists of C-language, using UNIX or UNIX based operating systems (Rafiee, R., Mahiny, A. S., Khorasani, N., Darvishsefat, A. A., & Danekar, A., 2009). Silva and Clarke (Silva, E. A., & Clarke, K. C. 2005) described it as a grid space of homogenous cells, with more neighborhoods of eight cells, two different cell (urban/non-urban states) and most importantly, five factors controlling the behavior of growth namely: diffusion, breed, spread, slope resistance and road gravity. Apart from the factors, the model also considers growth rules categorized into four broad types: spontaneous growth, new spreading Centre growth, edge growth and road-influenced growth. The factors can be calibrated according to the input layers provided and region under study. SLEUTH model has been extensively used because of its excellent compatibility, availability of open source files and demo data sets to execute the program (Project Gigalopolis) and better accuracy testing methods. Due to this, CA-SLEUTH model where used for this study, which has been widely used in the world, for modeling urban growth.

1.2 Statement of the Problem

Urbanization and urban growth are complex systems concerning social, economic, technological, and political forces interacting together. Given the increasing attention and rapid developments in built-up area expansion, an in-depth review of its progress and prospects is needed. According to UN DESA (2017), the global population which is more than 7.6 billion will grow to roughly 10 billion over the next three decades. Worldwide, urbanization in the form of urban sprawl is driven by increasing population figures resulting from the industrial revolution. At any rate, the policy makers and those that enforce land use regulations have been confronted with the reality of the negative impacts that accompany large-scale urbanization concerning both physical and human geography, including global warming, declines in habitat and biodiversity, and public health issues. To counteract the severity of effects, many governments have adopted "smart growth" of cityscapes, which emphasizes the construction of compact cities that favor a higher number of people per land unit as opposed to outward expansion that requires transportation network extensions (Rahimi, 2016; Sun et al., 2007). There is a call for urban change models formulated according to the development trends of specific cityscapes that can forecast future land cover scenarios (Curtis, 2018; Guan et al., 2011; Rahimi, 2016; Sun et al., 2007). Since worldwide urban population and built-up area show significantly divergent spatiotemporal pathways throughout much of noted urbanization process (Gao and O'Neill, 2021; Kuang et al., 2021), there is evidence that the imbalance between urban expansion and socioeconomic growth has tended to go up during the past several decades, especially in in developing country (Kuang, 2020). Therefore, it is an urgent priority to provide reference about sustainable urbanization, given that limited knowledge of urbanization sustainability dynamics in the next decade has been the primary challenges to inform the fulfillment of indicators.

In Ethiopia, Some studies have been attempted to analyze urban growth and its response to the landscape in the study area. For instance, Wondrade, N et al., (2014) analyzed urban growth and sprawl in Hawassa during the period of 1987 to 2012 and observed the tendency of urban sprawl in the city. Sinha P, Verma NK & Ayele E. (2016) quantified the urban growth of Adama using Landsat images from 1984 to 2015 and reported that the built-up area of the city increased by rapidly .Woldegerima T, Yeshitela K, & Lindley S. (2017) characterized the urban structure of Addis Ababa through urban morphology types and reported that the rapid urban expansion had occurred in the green space. Jenberu AA, and Admasu TG (2020) explore the driving forces of urbanization, land use pattern, and its challenges in Arba Minch town and reported that the town is in a state demographic and physical growth. Getu, K., & Bhat HG (2021) tried to assess and monitor the spatiotemporal dynamics of urban sprawl and its growth pattern in Bahir Dar and stated that the built-up area increased at the expanse of cropland and forest and also existence of sprawl with high dispersion. Those mentioned researches focused only on historical urban growth and didn't consider the future urban growth pattern. Modeling of urban growth provides better understanding of causes and mechanisms governing urban growth; to analyze alternative urban growth consequences. Therefore, modeling is important to support the appropriate urban planning and decision making responses to urban growth (Berling-wolff & Wu, 2004; Lambin et al., 2000; Li, 2011).

Additionally, from researches conducted on urban growth (Barow I, Megenta M & Megento T. 2019, Mekonnen Y & Hailu A. 2020), there is still specific knowledge missing as most of these studies had viewed urban growth in terms of land composition or only change in urban spatial extent. Analyzing the spatial extent and identifying the growth direction alone does not give sufficient insight in to the patterns of urban development processes, which are important to better understand urban growth pattern (Bishop MP., & Giardino JR. 2021), to bring this gap spatial configuration indices required.

On the other hand, the studies focused on simulating future urban growth with single planning period (Bekalo, MT, 2009, Woldegerima T, Yeshitela, K. & Lindley, S, 2017, Mekonnen Y & Hailu A ,2020, Getu K. & Bhat HG,2021). Besides, multiple future growth scenarios could be explored and simulated. At the moment, most of the simulations are based on trend scenarios, which provide useful insights as indicated in the work, but the sleuth model has the potential to do more. The scenarios are used to simulate possible spatial consequences of future urban growth considering specific planning conditions (Yang X; LoC, 2003) and to create effective strategies for a desirable future growth (Newman G; Lee J; Berke P, 2016). There for, this study was aimed at filling the existing gap by analyzing and modeling future urban growth of Assosa city using SLEUTH model considering alternative scenarios (business as usual, planed growth and environment-protecting scenarios) which can be milestone for sustainable development of Assosa city. Finally this study would assist planners and prospective stakeholders in planning a new heading before adverse effects become unavoidable.

1.3 Objectives of the Study

1.3.1 General objective

The general objective of this study was to model the historical spatial expansion and predict the future possible extent of urban growth in Asssosa City using SLEUTH Model.

1.3.2 Specific Objectives

The Specific objectives of this study are to:

- Analyze the changes in land use land cover in Assosa city from 1990 to 2021.
- Examine the dynamics of landscape structure in the study area from 1990 to 2021.
- Analyze the types of urban growth in the study area from 1990 to 2021.
- Model the historical spatial expansion of built-up area in Assosa City.
- Predict future urban growth in Assosa City under business as usual, planned growth, and environmental-protecting scenarios.

1.4 Research questions

This paper answers the following research questions with Corresponding to the problem statement,

- How to analyze the land use land cover of Assosa city from 1990 to 2021?
- How to examine the dynamics of landscape structure in the study area from 1990 to 2021?
- What are the types of urban growth of the study area from 1990 to 2021?
- How to model the historical spatial expansion of built-up area in Assosa City.
- How to predict the future urban growth of Assosa city from 2021 to 2050 under business as usual, planned growth, and environment-protecting scenarios?

1.5 Significance of the Study

This study aims to offer valuable information regarding the past and future changes on the urban growth of the study area. The findings of the study will be used by urban planners, government policymakers, urban and rural land managers, environmental experts, and other concerned bodies for their decision-making processes related to how urban dynamics through time. Additionally, it will be used as a reference for further studies related to analysis and modeling urban growth over time.

1.6 Scope of the Study

This study deals the spatiotemporal urban growth of Assosa City, in the Benishangul Gumuz Regional States of Ethiopia. This research focuses mainly on urban growth dynamics analysis from 1990 to 2021 and the future urban growth is modeled using the geospatial technology and SLEUTH model for the year 2050 and this gives information about urban growth to develop urban land use maps for the purpose of urban planning of Assosa city.

1.7 Limitation of the study

This study has following limitations: time constraint, financial constraint, data availability, and data quality like Lack of high resolution satellite data. In addition to this there is no Empirical study on urban growth modeling for the study area (published).

1.8 Organization of the Study

The study has organized in to five chapters. The first chapter contains brief description of introduction. The second chapter deals with literature review and addresses the relevant literature that was associated with the study. The third chapter has described the materials and methods. The fourth chapter was concerned with results and discussion of the study. Finally, the fifth chapter covers the conclusion and recommendations.

CHAPTER TWO: REVIEW OF RELATED LITERATURE

2.1 Introduction

Since the emphasis of this study is about spatiotemporal analysis and modeling the urban growth process, this chapter reviews the literature regarding urbanization and urban growth. The key concepts related to the urban growth were explained. After that, the related methods in the analysis and modeling urban growths also assessed.

2.1.1 Urbanization and urban expansion

Urbanization is simply defined as "the movement of people from rural to urban areas with population growth equating to urban migration" (United Nations, 2005). Urbanization is also a social process which involves the changes of behavior and social relationships as a result of people living in urban area (Bhatta, 2010). Essentially, it involves the complex change of life styles which result from the impact of cities on society (Bhatta et al., 2010). Nowadays, however, urbanization is commonly used in more broad sense and it refers to much more than simple urban population growth; it involves the physical growth of urban areas as well as the changes in the socioeconomic and political structure of a region as a result of population immigration to an urban area (Cohen, 2004; Deng et al., 2009; Li et al., 2013a).

Urbanization has been a dynamic complex phenomenon taking place all around the world. This process, without a sign of slowing down, has led to the significant changes in land cover and landscape pattern (Braimoh & Onishi, 2007; Deng et al., 2009). Dramatic urbanization, especially in the developing countries, will continue to be one of the important issues of global change influencing the human dimensions (Deng et al., 2009).

Associated with the process of rapid urbanization, the spatial expansion of built-up areas has been accelerating. Though urbanization promotes socioeconomic development and improves quality of life, urban growth inevitably results in significant land cover changes in urban area, such as the conversion from the forest and wetlands into agricultural or built-up lands since more land is used for the production of goods and services, and more residential land is required for the people living in the urban. While urban areas currently cover only 3 % of the Earth's land surface (Dewan & Yamaguchi, 2009), the conversions resulted from the urban growth are among the most significant types of anthropogenic land cover dynamics, and the ecological and environmental impacts of urban growth go far beyond the urban boundaries (Wu et al., 2011; Liu & Lathrop, 2002). This is particular the case in the fast developing regions where land cover change caused by rapid urban growth resulted in serious issues threatening urban sustainable development, for example, local and regional climate change (Kaufmann et al., 2007), hydrological circle alteration (Barron et al., 2013; Yang et al., 2011), forest loss and fragmentation (Miller, 2012) .

2.2 Analyzing of spatiotemporal dynamics of urban growth

2.2.1 Land use land cover change

Mapping and monitoring land use land cover have been widely recognized as an important step to better understand and provide solutions for social, economic, and environmental problems (Adb El-Kawy et al., 2011; Dewan & Yamaguchi, 2009b; Foody, 2002). Therefore the continual, historical and precise information of land use and land cover change is becoming increasingly important for urban planning towards sustainable development (Barnsley & Barr, 1996; Ramankutty & Foley, 1999).

Although most of the developed countries are well equipped with detailed land cover information (Dewan & Yamaguchi, 2009b), Longley and Mesev (2000) argued that the current understanding of the land cover change and its effects are largely limited by the lack of accurate and timely land cover data in the developing countries. Land cover data are inadequate or unavailable, of inconsistent quality, and out of date; while generating it is time consuming and expensive (Haack & English, 1996). This is attributed to the difficulties in accessing some regions because of equipment or funds to collect information properly, lack of trained personnel; or rapid changes (Defries & Townshend, 1999). With the wide requirement and application of land cover data, there has been an increasing interest in obtaining the data.

To understand the evolution of various land-use systems, to analyze dramatic changes of land use/land cover at global, continental, and local levels, and further to explore the extent of future changes, the current geospatial information on patterns and trends in land use/land cover are already playing an important role. Remotely sensed imageries provide an efficient means of obtaining information on temporal trends and spatial distribution of urban areas needed for understanding, modeling, and projecting land changes (Elvidge, et al., 2004).

2.2.2 Land Use Land Cover Change Detection

LULC change detection is finding changes in the features covering the ground through time. Nowadays, it is used to manage the impact of natural processes on climate variability (Story and Congalton, 1986). Additionally, it can help to monitor the long term effect of LULC dynamics on human life and environmental change (Congalton, 2009). LULC change can be detected using different techniques by utilizing two classified maps of different years. Among these techniques post-classification comparison (PCC) is a method used to detect LULC change (Foody, 2002).

2.3 Driving factors of urban growth

It is important to understand several factors directly or indirectly contributing to urban growth. There has been an increasing interest in identifying and understanding the effects of the driving factors on urban land cover change because this knowledge is crucial not only for the development of spatial models (Arsanjani et al., 2013; Zheng et al., 2012), but also more important for effective urban planning and management strategies (Dubovyk et al., 2011; Thapa & Murayama, 2010; Wu & Zhang, 2012). What drives/causes urban growth?" has always been one of the most common research questions. Urban growth can be described by the complex interaction of behaviors and structural factors associated with the demand, technological capacity, social relations, and the nature of the environment (Lambin et al., 2001; Verburg et al., 2004a).Various factors and their effects on urban growth have been identified in previous studies. The selection of the factors that are involved in the specific analysis often relies on prior understanding of the underlying processes of urban growth. According to the literature review, these factors considered in studies of urban land cover change can be grouped into four classes namely natural factors, socioeconomic factors, spatial policies, and neighborhood factors.

2.3.1 Natural Factor

In urban environment, natural factors are associated with the suitability and costs of a location for development. Topography often determines the location of new urban area because flat areas are suitable for urban development (Li et al., 2013a). Each location has a specific soil characteristic that determines the production of agricultural vegetation. The good quality agricultural land is not suitable for urban development in order to sustain future food supply (Li & Yeh, 2000).

2.3.2 Socioeconomic Factor

Socioeconomic factors are the most important factors of urban growth. A wide range of urban growth studies are based on socioeconomic theory. Urban economists identify three underlying driving factors that contribute to the urban growth: population growth, rising household incomes, and accessibility improvement (Mieszkowski & Mills, 1993). Urban area must extent to a larger area to accommodate more people. In order to promote life quality, households need more living space as they become richer. In addition, they focus on the site characteristics of live space, including housing prices, level of services, quality of landscapes (Geoghegan et al., 1997; Mertens et al., 2000). Other than census based socioeconomic variables, accessibility also strongly affects urban growth (Hu & Lo, 2007; Linard et al., 2013). The improvement accessibility indicates faster and more convenient travel and lower commuting costs. Verburg et al. (2004a) pointed out that "the influence of the socioeconomic conditions in the region can be best characterized by the access that a location has to these facilities."

2.3.3 Spatial policies

Spatial policies at national or regional level have significant impacts on land cover change (Dieleman & Wegener, 2004). They define the legal regulations for future land uses (Barredo et al., 2003). In particular, spatial policies can affect the urban development in two aspects. One is to serve as an accelerating factor to promote more new development in areas planner or proposed for development (Cheng & Masser, 2003), and the other is as a constraint to limit the development within a specific region, for example, the conservational or protected areas (Long et al., 2012; Verburg et al., 2004a).

2.3.4 Neighborhood Factor

"Everything is related to everything else, but near things are more related than distant things." The neighborhood factor is related with the Tobler's (1970) first law of geography. Land cannot be developed independently at each individual location; land cove patterns nearly always show spatial autocorrelation caused by a number of attraction and repulsion forces (Overmars et al., 2003). It is especially important to consider the neighborhood effect due to the fact that urban development can be regarded as a self-organizing system (Verburg et al., 2004b). A large number of studies demonstrated that locations are more likely to be converted to urban area if they are surrounded by more urban land. Neighborhood factors are introduced to consider the possible effects of spatial interaction and neighborhood characteristics by different approaches. For instance, the proportion of urban land and some other land cover types in the neighborhood of a cell (Braimoh & Onishi, 2007; Hu & Lo, 2007; Long et al., 2012); distance to existing urban areas (Poelmans & Van Rompaey, 2009).

2.4 Urban growth modeling

Modeling of urban growth process is an important technique to provide a better understanding of causes and mechanisms governing urban growth; to analyze alternative urban growth consequences, therefore, to support the appropriate urban planning and decision making responses to urban growth (Berling-wolff & Wu, 2004; Lambin et al., 2000; Thapa, R. B., & Murayama, 2011). Models of urban growth can be applied to predict the spatial pattern of changes by addressing the question "where are urban growth taking place?" or the rates of change by addressing the question "at what rate are growth likely to progress?" These two questions are associated with the location issue and the quantity issue (Pontius & Schneider, 2001).

2.5 Methods of Urban Growth Modeling

Urban growth geo-simulation models typically stem from research that combines multiple geospatial analysis methods, including satellite remote sensing (RS) and geographic information systems (GIS). The process of geo-simulation entails the comparison of two RS images from different points in time to interpolate a prediction of future conditions with a meaningful scheme of land cover classes derived from a time series of RS images, classified using methods such as Gaussian maximum likelihood and object-based image analysis (Rahimi, 2016). The subsequent classification is utilized in conjunction with a predictive geostatistical interpolation method to forecast future conditions.

Geostatistical methods that drive geosimulations can be identified as either empirical/statistical, dynamic machine learning-based, or agent-based (Guan et al., 2011; Rahimi, 2016). Typically, such models accept input for urban growth modeling in the form of rasterized land cover classifications and predictor geographic gradients. A typical land cover classification scheme includes agriculture, forests, urban areas, roads, water, and other lands, while typical predictor gradients include distance to roads, distance to urban centers, and population density. The focus of this paper is to review models that I found to be unique throughout an exploration of research collections available on the Internet and that are either solely dynamic, including artificial neural networks (ANN) and cellular automata (CA), or a combination of both empirical/statistical and dynamic in their process; namely the Markov

Chain. An ANN is a dynamic computerized model that attempts to duplicate human actions and learning functions. CA is a dynamic rule-based system where implicit raster cells represent the study area and time is represented as a series of adjacent steps (Sun et al., 2007). CA models move from one state to the next in an attempt to determine the state of each cell in a matrix according to the majority of a cellular neighborhood and the "weight" of each cell type in that neighborhood pertaining to transition potential (Guan et al., 2011). New CA models such as URBANISM, UPLAN, and SLEUTH have been evolved in recent years to forecast future changes trends of urban development both current and future, and to explore the potential impacts of different policy scenarios (Al-shalabi et al., 2013).

2.6 Sleuth urban growth model

Clarke and colleagues developed an urban growth model called SLEUTH based on cellular automata for simulating historical urban and land-use change (Clarke et al., 1997). The initial application of SLEUTH was successfully implemented in the San Francisco Bay area in simulating historical urban development (Clarke & Gaydos, 1998). The name of the model came from the six input data layers, namely Slope, Land cover, Exclusion, Urban extent, Transportation, and Hillshade. It is a program written in programming language C under UNIX that uses the standard GNU C compiler (gcc) and runs under Unix, Linux and Cygwin, a Windows-based Unix emulator (Project gigalopolis, 2003).

The model works in a grid space of homogeneous cells, with a neighborhood of eight cells, two cell states (urban/non-urban) with five transition rules that applied in consecutive time steps. The model can classify urban/non-urban dynamics as well as urban land use dynamics. These capabilities led the model to the development of two subcomponents within the model; an urban growth model (UGM), and a LULC change model or Land Cover Deltatron (LCD) (Dietzel & Clarke, 2007). Each subcomponent uses the same calibration phase, however, if only urban growth is analyzed, then Land Cover Deltraton is not stimulated by the model. It was only activated when land use/land cover is being analyzed by the model.

The model functions with predefined growth rules and uses the five factors to calibrate the model to a particular city. The rules of the model are complex than those of a typical cellular automaton (CA) and involve the use of multiple data sources such as transportation networks, topography, and existing land use details (Clarke et al., 1997). The growth rule where applied on cell by cell basis and the cell is updated at the end of every year.

2.6.1 SLEUTH model parameters

Urban growth in SLEUTH is modeled in a spatial two-dimensional grid and the basic growth procedure is a cellular automaton. The model simulates four types of urban land-use change: a spontaneous growth, a new spreading center growth, edge growth and road-influenced growth (Jantz et al., & Shelley, M. K., 2004). These growth types or rules are applied sequentially during each growth cycle, or year, and are controlled through the interactions of five growth coefficients: Diffusion (dispersion) coefficient, Breed coefficient, Spread coefficient, Slope coefficient, and Road gravity coefficient.

Spontaneous growth randomly selects potential new growth cells for urbanization. This means that any non-urbanized cell on the matrix has less probability of becoming an urbanized cell in any time step. This growth rules determined by the dispersion coefficient and slope coefficient which determines the weighted probability of the local slope. The stochasticity of the process is indicated by random. The cell state will not change if the cell is already urbanized or omitted from urbanization, and the ability to change also depends on the current cell value. (Project gigalopolis, 2003).

Diffusive/new spreading center growth determines the occurrence of new urbanizing centers by generating up to two neighboring urban cells around areas that have been urbanized through spontaneous growth. The breed coefficient determines the likelihood of newly generated urban pixels along with the road networks which begin its growth cycle.

Edge or Organic growth dynamics define the part of the growth that twigs from existing spreading centers. Edge growth is controlled by the spreading coefficient which stimulates the probability that nonurban cell with at least three neighbors will also become urbanized. Road-influenced growth is determined by the existing transportation networks on growth patterns by generating new spreading centers adjacent to roads.

Newly urbanized cells are randomly selected which is determined by the breed coefficient. The accessibility of road locations attracts urban development. According to Clarke et al. (1997), the most prevalent type of urban growth during the model run is recorded as an organic growth type, followed by spontaneous growth. It was noted that road-influenced growth increases as road layers from different historical periods are read in at the correct time.

The above growth rules are influenced by the five growth factors applied in the SLEUTH model. These controlled values are calibrated by comparing simulated land cover change to a study area's historical data (Project gigalopolis, 2003). The diffusion factor controls the depressiveness of isolated urban pixels which was generated by spontaneous growth. A breed factor controls the new spreading growth and the road gravity growth by monitoring the probability to become another newborn urbanized pixel of urban growth center and along the road influenced growth.

A spread factor controls the edge/organic growth type whether additional growth can be offspring from old or new urban centers. The breed coefficient controls the new spreading growth and likelihood of growth occurring along with the road networks. The slope resistance coefficient influences the likelihood of settlement development on steep slopes. A high slope coefficient value will decrease the likelihood of urban development that will occur on steep slopes. Road gravity factor attracts new settlement towards and along with the existing road system. The coefficient determines the maximum probing distance of selected urban cells.

2.7 Empirical Literature Review

The empirical study of urban spatial growth is accessed from internet sources and same published research. Few of them have been presented in the following. From the review, it was understood that Analyzing and modeling of urban growth needs more investigation to understand urban dynamics.

Because of urban growth results in tremendous urban land cover change, many researchers have made progress towards an accurate definition by evaluating land use and land cover change (LUCC) in urban areas (Bagan & Yamagata, 2012; Banzhaf et al., 2009; Serra et al., 2008; Yuan et al., 2005). With spatiotemporal analysis of remote sensing image, LUCC change can be detected quantitatively, which will help researchers identify clearly how and how much different urban land cover patterns have changed during a time period. However, during the process of urban growth, land cover pattern change is just one indicator of the changes that have occurred. Merely describing different urban land cover pattern change cannot identify urban growth dynamics precisely.

Researchers have developed an urban growth measuring model by combining spatial indices with socio-economic indices (2007; Jiang et al., Huang et al., 2009; Jiang et al., 2013). Jiang et al. (2007) indicated that the causes, evolution, and consequence of landscape pattern change should be discussed with spatial indices. In their study, Jiang et al. (2007) focused on three indices to measure urban growth in Beijing, China: shape index, area index and leapfrog development index. Their study showed that using those indices can effectively reduce the interpretation difficulty in urban growth pattern. However, it also relies extensively on ancillary data such as socioeconomic data.

Many studies have used landscape metrics to evaluate urban spatial growth patterns (Batisani & Yarnal, 2009; Feng & Li, 2012; Jat et al., 2008; Xu & Min, 2013). Landscape metrics are primarily used for urban ecology investigation because they can show the urbanization process through the changing landscape form, and can be adopted to analyze the urban landscape pattern change in a certain time period. Schneider and Woodcock (2008) note that landscape metrics are an effective approach to better understand urban configuration, especially now that the trend of urban landscape change usually begins with the extension of a plot. Numerous landscape metrics can be used for the study of landscape distribution. However, many of them are highly correlated to each other and thus provide redundant information, which will impact the result of research (Bhatta et al., 2010a; Schneider & Woodcock, 2008). Thus, in order to reduce information redundancy, carefully choosing landscape metrics is essential.

Modeling and simulating spatial urban growth patterns are required to better understand the complexity inherent in the urban growth process and its influence on land cover change. The SLEUTH model provides one such tool that allows for simulating future urban growth and land use change necessary for land use management. Pankaj et al, 2019 used the SLEUTH model to examine the impact of urban development on three major development areas. Bajracharya, P., Lippitt, C. D., & Sultana, S. (2020) also used this model in Albuquerque, New Mexico, based on the past pattern of urban growth and development that has occurred in the city. Chaudhuri & Clarke (2013) examined The SLEUTH Land Use Change Model: A Review Over the last 15 years, since its first publication, SLEUTH has continuously been explored, modified and applied worldwide by the land use change modeling and planning communities. Over these years, one of the biggest criticisms and yet a strength of SLEUTH is its simplicity, which has led to an increasing number of applications. The SLEUTH model helps to create different future urban growth scenarios by changing the input data or modifying the coefficients of the model (Dietzel and Clarke, 2007). Li et al , (2018) concluded that the SLEUTH model can be used as an important planning tool to incorporate different urban development factors into future urban growth projection. A number of studies have incorporated policy planning and environmental quality into the model to achieve connection of the SLEUTH model with other data sets or methods (Sakieh et al., 2015; Han et al., 2015 and Butsch et al., 2017).

The spatiotemporal patterns and dynamics of urban growth had been a consistently discussed topic in urban studies. With increasing acceptance of the concept of smart growth and sustainable development, scholars had paid renewed attention to urban growth (Wei et al., 2014). However, there is a scarcity of research on integrating different scales of analyses on urban growth types and functions remain largely undone. Using Assosa City as a case, this study quantified and highlighted the spatiotemporal patterns, growth types, and future possible urban extent of the area. This could provide a case to further understand urban growth in fast-growing cities in Ethiopia like Assosa city, which is both timely and necessary.

2.8 Research and Knowledge gaps

Although many studies on urban growth were conducted in the past years there is still specific knowledge missing as most of these studies had viewed urban growth in terms of land composition or only change in urban spatial extent. Analyzing the spatial extent and identifying the growth direction alone does not give sufficient insight in to the patterns of urban development processes, which are important to better understand urban growth pattern (Bishop MP, & Giardino JR, 2021), to bring this gap spatial configuration indices required. Besides, multiple future scenarios could be explored and simulated. At the moment, most of the simulations are based on trend scenarios, which provide useful insights as indicated in the works so far, but the sleuth model has the potential to do more. The scenarios are used to simulate possible spatial consequences of future urban growth considering specific planning conditions (Yang X and Lo C, 2003) and to create effective strategies for a desirable future growth (Newman G, Lee J, Berke P, 2016). Even though Ethiopian cities share many of the urban growth characteristics (discussed in the statement of the problem section), more research is needed to examine the extent to which the evolving spatial structure of cities and Assosa City’s to.

2.9 Conceptual framework

This study makes use of both remote sensing and spatial metrics methods to get an understanding of spatiotemporal urban growth process and the underlying patterns. The conceptual framework is composed of three major elements interacting at different stages of the study. Those are remote sensing, spatial metrics and predicting urban growth using SLEUTH model. The first one shows the potential use of classified temporal remote sensing image to detect the LULC change of the study area. The second shows interaction between urban remote sensing and spatial metrics computation in Fragstatst to quantify urban landscape fragmentation patterns. Following the LULC analysis, landscape metrics for each time series maps were calculated. This metrics are computed to quantify the spatial configuration and composition of urban landscape, from this spatio-temporal urban growth patterns were determined. Moreover this study summarizes the prediction of future urban growth with three scenarios (business as usual, planned growth and environment protection scenarios) with the help of SLEUTH model.

CHAPTER THREE: MATERIALS AND METHODS

3.1 Description of the study area

3.1.1 Location

Assosa city, the capital seat of Benishangul Gumuz region is one of the cities in the country having a great natural potential, competitive and comparative advantage of development. Assosa is located in western extreme part of Ethiopia about 687km from Addis Ababa in Benishangul Gumuz Regional State. So, the city could be taken as one of the border city in the country and located at 90 km away from the Ethio-Sudanese border. It is situated on a flat plane at an average altitude of 1,550 m. msl (MWR, 2001). The town geographically located between 10°00' and 10°06' north and between 34°35' to 34°39' east. The area can be accessed through ground and air transportation. The ground access is via Ambo- Nekemte-Gimbi-Nejo-Mendi-Bambasi and then to the study area (Assosa).

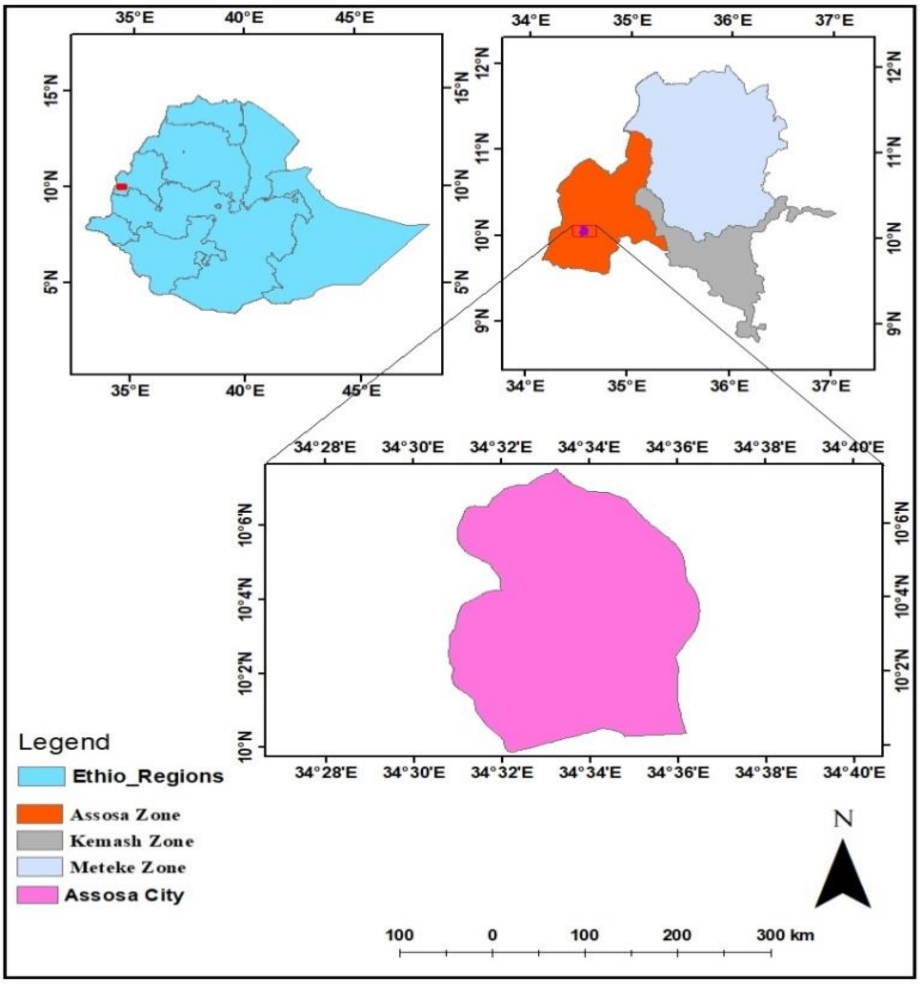

Figure 3.1: Location map of the study area

3.2 Data Used in This Research

This research was conducted using Landsat images as the prime remote sensing data due to the availability of images for an extensive period of time as compared to other satellite types. Four Landsat images (1990, 2000 2010 and 2021) were obtained from the United States Geological Survey (USGS) online data portal, for the purpose of generating LULC each perspective years of the study area. For the purpose of extracting slope and hillsides of the study area Free ASTER image was used.

Basically, the satellite images were selected based on the availability of data and quality. For this reason, this study uses Landsat 30m resolution to extract LULC and road networks of the study area. Several ancillary data were also collected for this research. GPS coordinates were collected using hand held GPS for the purpose of validation of the classification. Administrative boundaries were obtained from the Assosa city land administration office. All of the datasets used in the study were geometrically calibrated using adindan UTM zone 36 North projections.

Table 3.1 Characteristics and properties of the Landsat images used in this study

Acquisition Date	Path/Raw	Sensor	Spatial resolution
14/06/1990	171/ 53	TM	30m
06/05/2000	171/ 53	ETM+	30m
12/01/2010	171/ 53	TM	30m
24/ 04/2021	171/ 53	OLI_TIRS	30m

3.3 Software used

In order to achieve the objectives of this research the following Software were used. Arc GIS is used for spatial information analysis. ENVI 5.3 is used for image preprocessing and classification. Fragstsats 4.2 is used to quantify urban growth pattern. SLEUTH Model is also used to simulate and forecast future urban spatial growth for the study area. Table 3.2 shows the implemented software, lists with their corresponding version and purposes.

Table 3.2 software used in this research

Software used	Its functions
ArcGIS (10.8)	For analyzing spatial information
ENVI 5.3	Image preprocessing and classification
Cygwin	To simulate and forecast future urban spatial growth
Fragstat 4.2	Spatial metrics analysis

3.4 Method of Data Analysis

The analyses of this research were conducted to map urban built-up areas based on the satellite images and using other ancillary data. By delineating with the city boundaries, the spatial patterns of urban growth trends were analyzed and quantified using landscape metrics. The future urban growth trends also predicted with the help of CA-based SLEUTH model. Overall methodological flowchart is indicated in figure 3.2.

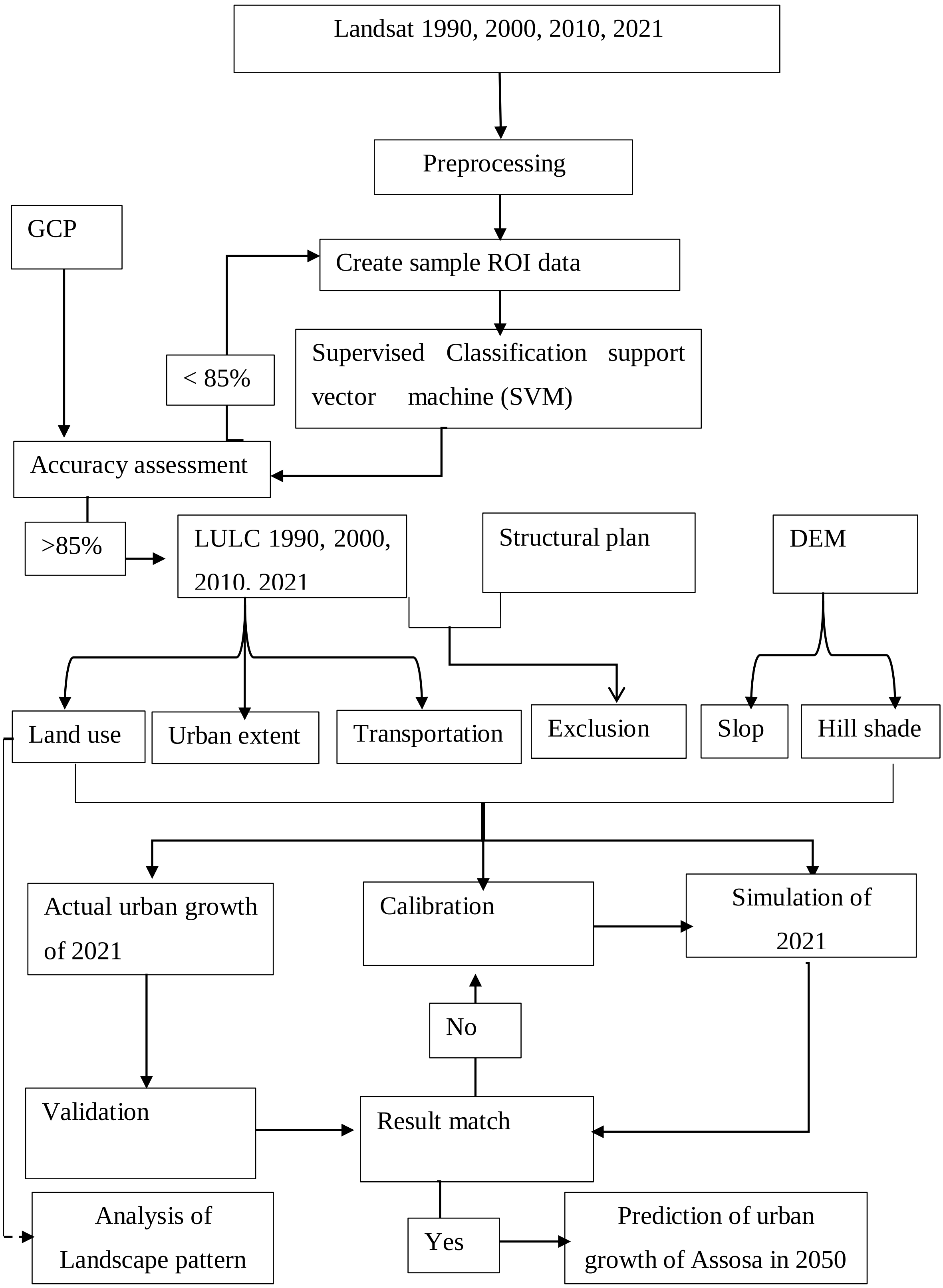

Figure 3.2: Methodology flow chart

3.5 Analysis of land use land cover changes

Land cover change denotes a change in certain continuous characteristics of the land such as vegetation type, soil properties, and so on, whereas land-use change consists of an alteration in the way certain area of land is being used or managed by humans (Patel et al., 2019). This involves the transformation in the natural landscape due to urban growth. It is interesting to note that this change is responsible for a number of local and global effects, including biodiversity loss and its associated effects on human health, and the loss of habitat and ecosystem services (Patel et al., 2019). It is mainly driven by urban growth and is particularly important now for developing and underdeveloped countries. However, natural causes may result in land cover change, but land-use change requires human intervention (Joshi et al., 2016). In this study The LULC features are extracted from Landsat images using the SVM algorithm of supervised image_classification technique in ENVI 5.3 software.

3.5.1 Image classification

Image classification is widely used in several Remote Sensing applications for extracting thematic information. It combines pixels into more representative represent similar land features (Jensen, 1996). Classification requires an explicitly formulated algorithm for various purposes as it is highly dependent on the objective required.

Unsupervised classification: pixels with collective characteristics are clustered without the aid of the analyst. Once the number of classes is specified by the user, the software fixes which pixels are associated with and assembled them into classes. The analyst specifies the algorism used in the software and the variation within each category (Benayas et al., 2007).

Supervised classification: the analyst collects training samples from each category and orders the software to classify the remaining pixels accordingly (Perumal and Bhaskaran, 2010). Once the training samples were collected, the image was classified according to the selected algorithm.

3.5.2 Land-Use Land-Cover Classification Scheme

Open access Landsat images are widely used around the world to assess and quantify land-use/land-cover variations from the micro to mega level and to record human-caused interruptions (Yuan et al., 2005). Precise land-class and land-use change data for analytical purposes are difficult to obtain, especially in built-up areas due to their diversified land characteristics and mixed pixels (Perumal and Bhaskaran, 2010). Barren land and impermeable developed areas commonly present similar types of spectral reflectivity, which is confusing and makes it difficult to correctly differentiate between these two land-use types (Deilmai et al., 2014). The first objective of the present research was to evaluate and detect the land-use/land-cover changes and spatial magnitude using spatiotemporal information. For this purpose, four types of land classes were proposed (Table 3.3). The land classes were prepared based on ground investigations.

Table 3.3 LULC classification scheme

LULC type	Description
Built-up	Houses, paved surface, road etc.
Farm land	Includes Cultivated lands
Forest	Natural vegetation and plantation
Barren land	Includes a surface with no or little vegetation, open land, exposed soil, rock, grass land etc.

3.5.3 Classification algorithm

For this study, four multi-temporal medium resolution Landsat images are used to analyze the urban growth trends and patterns of Assosa city for the past 31 years. As described in section 3.2, all images are acquired geometrically corrected and geo-referenced. Owing to its popularity and wide acceptance in remote sensing image classification, supervised classification with support vector machine (SVM) algorithm in ENVI 5.3 software environment was applied. SVM is a non-parametric classifier. Unlike parametric classifiers such as maximum likelihood which assumes that the data is normally distributed, non-parametric classifiers do not base classification on a normality assumption or statistical parameters (Phiri and Morgenroth, 2017). Because highly heterogeneous land covers data (e.g., urban areas) are unlikely normally distributed, the distribution of land cover surfaces is associated with various uncertainties which prevent their description based on data distribution (Lu and Weng, 2007). In this respect, non-parametric classifiers provide better results as compared to parametric classifiers in complex landscapes. Accordingly, each image was classified in to different land cover classes which finally ended up generating four different year land-cover maps of the study area.

3.5.4 Accuracy assessment

Accuracy assessment was used to validate the classification by assessing how pixels were assigned to the correct Land use land cover classes. The main purpose of assessment is to assure classification quality and user confidence on the product (Foody, 2002). Google Earth's historical satellite image and ground truth data collected from the field were used to assess the accuracy of classification. Accuracy of the classification results for the year 2021 was assessed using 244 randomly sampled ground truth points, obtained from fieldwork. However, since it has been difficult to get reference data for accuracy assessment of image 1990, 2000, and 2010, visual interpretation of Google Earth and the true color composite of the Landsat images were used.

The overall accuracy identifies the percentage of correctly classified pixels from the total pixels. But it misses how errors are distributed across each LULC category. To indicate this, the producer's accuracy and user's accuracy were applied. User's accuracy is the ratio of correctly classified pixels to classified total. Whereas the Producer's accuracy is the ratio of correctly classified pixels to Reference total pixels.

The Kappa Coefficient is generated from a statistical test to evaluate the accuracy of classification. Kappa essentially evaluates how well the classification performed as compared to just randomly assigning values, i.e. did the classification do better than random. The Kappa Coefficient can range from -1 to 1. A value of 0 indicated that the classification is no better than a random classification. A negative number indicates the classification is significantly worse than random. A value close to 1 indicates that the classification is significantly better than random (Jennes et al (2007). Kappa is a statistical measure of overall agreement between two maps (e.g. output of classified/simulated map and ground truth/reference map) or a matrix (Canada Centre for Remote Sensing, 2010). Kappa coefficient can be calculated using the below formula:

K= $\frac{N\sum \mathrm{Xii}-\sum(\mathrm{Xi}*\mathrm{Xj})}{(\mathrm{N}*\mathrm{N})-\sum(\mathrm{Xi}*\mathrm{Xj})}$ $k = kappa\ coefficient$, N= $Total\ number\ of\ pixel\ points$, xii = $correctly classified\ points\ in\ column\ i$, xi = $sum\ of\ row\ points$, xj = $sum\ of column\ points$.

Table 3.4 Category of Kappa Statistics

Kappa statistics	<0.00	0.00-0.2	0.21-0.40	0.41 – 0.60	0.61 – 0.80	0.81 – 1.00
Strength of agreement	poor	slight	Fair	Moderate	Substantial	Almost Perfect

Source: Congalton and Green (2009)

3.6 Land use Land cover change detection

The LULC changes were detected between two pairs of LULC maps between 1990 and 2021. Change detection is the process of identifying differences in the states of an object by observing it at different times. Image differencing, principal component analysis and post classification detection are the most widely used methods for change detection (Lu et al., 2004). The detections were held between the years (1990 – 2000, 2000 – 2010, and 2010 – 2021). Using post-classification comparison techniques the area of each LULCs were identified.

3.7Analysis of Landscape pattern and its dynamics

The processes of urbanization usually change the landscape pattern in urban regions. Such changes are mostly accompanied by decreasing the heterogeneity of landscape compositions and increasing landscape fragmentation by generating smaller patches (Yeh & Huang, 2009). Spatial metrics are useful tools to quantify the dynamic patterns of ecological processes. Changes in urban landscape pattern can be detected by using spatial metrics that quantify and categorize complex landscapes structure into simple and identifiable patterns.

3.7.1 Selection of spatial indices

Based on the work of O'Neill et al (1988), a number of different metrics were developed, modified, and investigated (for example, Li and Reynolds, 1993; McGarigal and Marks, 1994). The most commonly used metrics are Class area (CA) ,number of patch(NP), patch density(PD), largest patch index (LPI),edge density(ED), area waited mean patch fractal dimension(WMPFD), Shannon’s evenness index , contagion index and the fractal dimension. For this specific study selected metrics has been used. From spatial landscape metrics the type of urban growth pattern is determined. The FRAGSTATS software package was used to quantify landscape patterns and their changes for the study area. The FRAGSTATS has been widely used in landscape ecology and land fragmentation analysis (Reed, Johnson-Barnard et al. 1996, Keleş, Sivrikaya et al. 2008). Among various pattern indices calculated by FRAGSTATS, i selected five commonly used measurements to characterize spatial patterns of urban built-up area: the total number of patches (NP) , patches density (PD), edge density (ED), the largest patch index (LPI), and the area weighted mean patch fractal dimension (FRAC_AM/AWMPFD). The detail of the metrics used in this study is listed in table below.

Table 3.5 Description of spatial metrics used in this study

Metrics	Description	Units	Measure of
NP	The number of urban patches is the measure of discontinuous urban areas or individual urban units in the landscape.	None	Diversity or richness of the landscape.
PD	PD equals the number of patches of a specific land cover class divided by total landscape area.	No./ 100 ha	fragmentation
ED	The sum of the lengths of all edge segments involving a specific class, divided by the total landscape area multiplied by 10000.	Meters/ ha	fragmentation
LPI	The area of largest patch of the corresponding class divided by total area covered by that class, multiplied by 100.	Percent	dominance
AWMPFD	It describes the complexity and fragmentation of a patch by a perimeter-area ratio. Lower values indicate compact form of a patch. If the patches are more complex and fragmented, the perimeter increases representing higher values.	None, range: 1-2	fragmentation and complexity

Source: McGarigal, K. (2015)

3.7.2 Change detection in landscape patterns

Several qualitative and quantitative methods were employed to analyze the spatial landscape pattern changes of land use at different stages. Here, landscape patterns were evaluated using landscape metrics, which can be calculated on the three different levels: patch, class, and landscape levels. In this study, class level metrics were employed. Class-level metrics are used to qualify the characteristics of the same LULC type and return a unique value for each class in the landscape. Landscape-level metrics return a unique value corresponding to the landscape mosaic as a whole (Pelletier et al., 2016). Landscape metrics selected in this study are provided in Table 3.5. To visualize the spatiotemporal changes in landscape patterns and reveal their temporal and spatial characteristics during urbanization, the LULC maps of the four years were obtained in this study. The landscape metrics at the class level for urban area were calculated using the Fragstats 4.2 software to analyze the spatiotemporal changes in the landscape patterns.

3.8 Analysis of urban growth type

Pattern-process analysis is one of the main threads in landscape ecological research, which aims at understanding the complex relationships between landscape patterns and landscape change processes (Schro¨der and Seppelt 2006). Resulting from interactions among different ecological processes and natural environments, landscape patterns can affect ecological processes in multiple ways, while ecological processes can facilitate the evolution of landscape patterns. One of such important ecological processes is landscape expansion (including urban growth, species spreading, desertification, soil erosion, etc.). It involves mainly three types of urban growth i.e., infilling, edge-expansion, and outlying, while other patterns can be regarded as variants or hybrids of these three basic forms (Forman 1995; Ellman 1997; Wilson et al. 2003).

An infilling type refers to the one that the gap (or hole) between old patches or within an old patch is filled up with the newly grown patch. Forman (1995) discusses edge-expansion type, defined as a newly grown patch spreading unidirectional in more or less parallel strips from an edge. If the newly grown patch is found isolated from the old, then it would be defined as an outlying type. In this study urban growth type is discussed using the results of landscape metrics discussed in section 3.7.

3.9 Modeling urban growth using sleuth

To predict the future urban extent of the study area Sleuth modeling method is used for this research. The SLEUTH urban growth model was calibrated using the multi-temporal data sets for the entire study region. The calibrated model allowed us to fill gaps in the discontinuous historical time series of urban spatial extent, since maps were available only for selected years between 1990 and 2021. This model also allows us a spatial forecast of urban growth up to the year 2050.

The sleuth model works using six parameter namely land use, urban extent, slope, exclusion, road (transportation) and hill shade. The model has three phases namely coarse calibration phases, fine calibration phase and final calibration phases. Using those six historical input data, the sleuth model predict or simulate the future growth patterns of the study area. The prediction phase considers scenarios for urban growth.

3.9.1 Input data for sleuth

SLEUTH model required at least five input datasets (or six, if land use is included). These layers are Slope layer, Land use, Exclusion layer, urban extent, Transportation network, and Hillshade layer. For statistical calibration of the model, at least four temporal urban extents, Minimum of two transportation layers from two different years and land-use layers from at least two periods along with each slope, excluded and hill shade layers are required on three spatial resolutions with the same coordinate system and extent. The model also requires a special naming format for the input datasets (Project gigalopolis, 2003).

Slope layers

Topography acts one of the important factors in urban development. Flat areas are more suitable for urban growth. In this research, the slope layer was prepared from the 30 meter spatial resolution of Digital Elevation Model (DEM). The layer was prepared in percentage values and then changed into integer value through reclassification from 0 to 255. Since the topography will not change dramatically in the short term, the same slope layer was used for model calibration and prediction scenarios.

Land use layer

An optional input layer to the SLEUTH model is a LULC. LULC with consistent classification for at least two periods is needed for the model. Each pixel value contained in the grayscale, land use images should represent a unique land class (Project gigalopolis, 2003). For example, the LULC class Urban is encoded by integer assigned as 1 and class Agriculture as 2 in order. Finally, they were transformed into GIF format.

Excluded layer

This constraint layer has an important role in urban growth by setting up resistant factors of urbanization (Qi, 2012). To what extent the excluded regions would be protected from the growth was indicated by assigning the numeric value (0 – 100). For example, while a value of 100 indicates that the area should be excluded from urban growth (100 % protection), 50 shows that only 50% of that area should be protected. Locations that are available for urban development have a value of zero. Concerning the areas designated by the policy plans, such as protected areas, wetlands, and open spaces, the values can be assigned based on the importance or priority of the development policy in the region. (http://www.ncgia.ucsb.edu/projects/gig).

With regard to areas delineated by policy and urban plans, such as unprotected wetlands, protected farmland or vegetable plots, values varying from 0 to 100 can be assigned on behalf of urbanization opportunities: the closer the value is to 0, the higher probability of urbanization; the closer to 100, the more unlikely to be urbanized. Hence， Excluded layer plays a significant role in SLEUTH modeling, and by adjusting it, a SLEUTH model can integrate urban planning, policy and other macro elements to forecast urban development from regional perspective.

Urban layer

For this study, four temporal datasets of urban the area from 1990, 2000, 2010, and 2021 have been extracted from satellite images. Urban layers are the base layer for running the SLEUTH model. The beginning year known as a ‘seed’ layer is used to initialize the model and other years called controlled layers are applied during model calibration phase for the least square calculation to obtain the goodness of fit statistic results. The model requires the binary classification of urban or non-urban data with a value of 1 indicating the urban and 0 indicates non-urbanized area. The land use layer is optional for SLEUTH model and was excluded from the modeling process.

Transportation layer

Transportation network has a great impact on urban development as the city tends to develop to the directions along with the transportation networks. The SLEUTH model requires at least two year transportation data to simulate dynamic effects of the model. In this case main rods of Assosa City for 1990, 2000, 2010, and 2021 were used.

Hill shade

This layer has no impact on the model simulation. It is used for better visualization as a background image to the spatial data generated by the model output files. This layer can be embedded with water bodies such as rivers and lakes to enhance the visual effects.

To run the SLEUTH model, input data need to be standardized in terms of data format, the same spatial resolution, and the same extents (rows x columns). Firstly, we need to convert all the layers into a single raster format in ArcGIS environment, and then resample each layer into three spatial resolution of 120 meter, 60 meter, and 30 meter respectively using the nearest neighbor algorithm. Then covert these images into an 8- bit GIF format and rename the files according to the naming convention followed to run the model (Project gigalopolis, 2003).

3.10 SLEUTH model implementation

3.10.1 Model calibration

Model calibration was done with SLEUTH version 3.0 beta with patch 1 obtained from the Project Gigalopolis web page. The model calibrate through Cygwin command which is a Linux based emulator that runs inside windows. Before running the calibration mode, test run is done in order to check if input data sets were correctly prepared as per the model requirement. The purpose of calibration is to obtain the best set of parameters to make the model capable of simulating a city with the best match with the real world scenario (Oguz et al., 2007). The calibration was performed in three phases; coarse, fine and final phases. Input data in 30 meters resolution were resampled into 120 meters to be used in the coarse calibration phase, into 60 meters to be used in the fine calibration phase. Data sets with 30 meters (full resolution) were used in the final calibration phase. These resolutions were applied due to the model's extensive computational demands, which are directly proportionated to the resolution of the data and the size of the area to be modeled (Watkiss, 2008).

In this study, the calibration phase encompassed the years from 1990 to 2021 and four urban extent map of the year 1990, 2000, 2010 and 2021 was utilized. In each phase, the coefficient range, increment size, and resolution of the input layers were changed. To find the best fit model, 11 different metrics were calculated for each run of the model. In this study, the shape factor called LeeSallee metric was used for choosing the best parameters set. The output statistics file was sorted by descending order using LeeSallee metric and the five highest scoring values and respective parameter values were selected.

Coarse phase: In this phase model parameters are widely defined. It is recommended to set to (0-100, 25), where the 0 is the start vale, 100 is the stop value, and 25 is the step (Project gigalopolis, 2003). This gives 3,125 (55) different parameter sets that are tested to determine which range of parameter sets that best describes the data located within the calibration phase. To reduce the computation time, a value of 4 is used for the number of Monte Carlo computations.

Fine phase: in this phase, it further narrow down the parameter ranges to about 10 or less (± 5) and it takes steps of 5 or 6 units through the coefficient space (Project gigalopolis, 2003) and more times of Monte Carlo iterations (number_of_times) was used to reduce the level of error. It was increased to 8 and the unit computation time also increases with a larger number of Monte Carlo iteration.

Final phase: Using the best-fit values found in the control_stats.log file produced in the fine calibration phase, the range of possible coefficient values is narrowed. The range is narrowed so that the increment of 1-3 may be used while using about 5-6 values per coefficient (eg, for a single coefficient, value = (4, 6, 8, 10, 12) and a larger number of Monte Carlo iterations (number_of_times) to 10 is used.

3.10.2 Model simulation

The urban growth and landscape change from past to present was simulated and projected to the future changes for different scenarios. The model simulation from past to present (1990 – 2021) would serve as a visual confirmation for the model calibration. It would also provide a historical view of urban growth and landscape change. For model simulation, the final derived coefficient values are used as the starting values for model simulation. In order to minimize the uncertainty in model simulation, higher value of 10 Monte Carlo iterations is used. The model simulation produces various statistical measures apart from the simulated images which will represent the general trend of urban growth.

3.10.3 Model validation

To assess the model accuracy is an important component of the predictive modeling especially if the models are to be used for the decision-making purposes (Abedini & Azizi, 2016). Different methods were used to assess the simulation accuracy. Sakieh et al. (2014) had used two separate validation indices; the receiving operator characteristic (ROC), and the Kappa index of agreement. Serasinghe et al. (2018) validated model performance by comparing the number of simulated pixels to the number of urban pixels in the urban extent layers, which was derived from satellite images using the maximum likelihood classification method. Similar validation was carried out by Oguz et al. (2007) and Abedini & Azizi (2016) through comparison of the simulated urban extent with the observed urban extent with the construction of error matrix and evaluating the overall classification accuracy and kappa coefficient (Oguz et al., 2007). Visual interpretation of the simulated urban growth with actual urban growth has been also used for judging the model prediction accuracy (KantaKumar et al., 2011). Other than graphic interpretation serving as a confirmation for the accuracy of the model, it also provides a historical perception of urban development and landscape change in the particular region (Yang & Lo, 2003).

In this study, the model validation was conducted by comparing the simulated results generated from the SLEUTH model with observed maps of the actual urban growth of the seed year. It is discussed that visual interpretation is also one of the important validation of model accuracy since it gives a visual idea about the different growth patterns and different land-use types if the land use land cover map is modeled. The accuracy of the models is judged by their predictive power (Silva & Clarke, 2002).

3.11 Prediction of future Urban Growth

The scenarios are used to simulate possible spatial consequences of future urban growth considering specific planning conditions (Yang X; Lo C, 2003) to calculate the potential impact of land transformation (Clarke K; Gaydos L,1998), and to create effective strategies for a desirable future growth (Newman G; Lee J.; Berke P,2016).

Scenario- based planning is the testing and application of different scenarios to come up with a plan. It is a powerful way to deal with uncertainties of the future associated with urban growth, and has been a common practice in recent years with technological advancements (Kamruzzaman, & Yigitcanlar, 2017).

The building of scenarios ('What If?') in the context of policy option for regional planning and governance turned out to be very appealing and stimulated the discussions more than graphs and text. The idea of this exercise is to bridge the two communities in order to collaborate around spatial models and produce future land use maps which should have a clear and accepted interpretation, be robust, statistically validated and respond to policy interventions. By using urban growth rate as a driving force, three scenarios were developed for this study. The first one is Business as usual: urban areas are expected to expand simply based on the previous growth pattern. The second scenario is planned growth scenario: future development as previously defined land use plan or plan policies. The last one is Environment-protecting scenario: Urban growth allocation was limited to the environmental considerations.

CHAPTER FOUR: RESULTS AND DISCUSSION

In the previous chapters, an attempt was made to illustrate the SLEUTH model functions that can study the urban growth using the historical datasets and how urban growth can be analyzed by adopting related methods. In order to evaluate the performance of the proposed methods described in previous chapter and for better understanding of the urban growth scenarios in the current study area, the methods have been applied and the findings of the study was discussed in this chapter in detail.

4.1 Spatiotemporal Land use land cover results

Land use land cover classification result of 1990 showed that the dominant LULC classes were farmland. This class accounted for 7062.61ha, which is 66.2% of the overall area coverage. From the total area of 10,667.69 ha, forest accounted for 2707.14ha (25.4%) and barren land accounted for 759.10 ha (7.1%). Area covered by built up for this year was 138.84 ha (1.3%). The built up and barren land covered the smallest area than all other classes. Analysis of 2000 image revealed that the farmland constitutes the largest proportion of the study area with the value of 5615.60ha (52.6%), followed by barren land, which accounted 3525.36 ha (33.1%). in this year the forest land covers 1290.79 ha (12.1%) and built-up area accounted for 234.14 ha (2.2%) of the total area. Land-use/land-cover classification results of 2010 image revealed that the dominant LULC categories were still the farmland and forest land together accounted for 90% of the total area. In this year the barren land accounted for 626.77 ha (5.9%) and Area covered by built-up were 436.08 ha (4.1%). Also the classification result of 2021 showed that forest and farmland holds the dominant class which is about 4349.63ha (40.8 %) and 3874.33ha (36.3 %) respectively. In this study period the built-up and barren land covered 1108.49 ha (10.4%) and 1335.24 ha (12.5%). However, the extent of Built-up area was increased by 970 ha within 31 years. Detailed statistical data for each of these classes and LULC map of the study period are shown in Table 4.1, Figure 4.1 and Figure 4.2.

Table 4.1: LULC classes and area coverage of Assosa city in 1990, 2000, 2010 and 2021

LULC class	1990		2000		2010		2021	
	Area (ha)	%	Area(ha)	%	Area(ha)	%	Area (ha)	%
Built up	138.84	1.3	236.84	2.2	436.8	4.1	1108.49	10.4
Farm land	7062.61	66.2	5615.60	52.6	5026.74	47.1	3874.33	36.3
Forest	2707.14	25.4	1290.79	12.1	4578.16	42.9	4349.63	40.8
Barren land	759.10	7.1	3524.36	33.1	626.77	5.8	1335.24	12.5

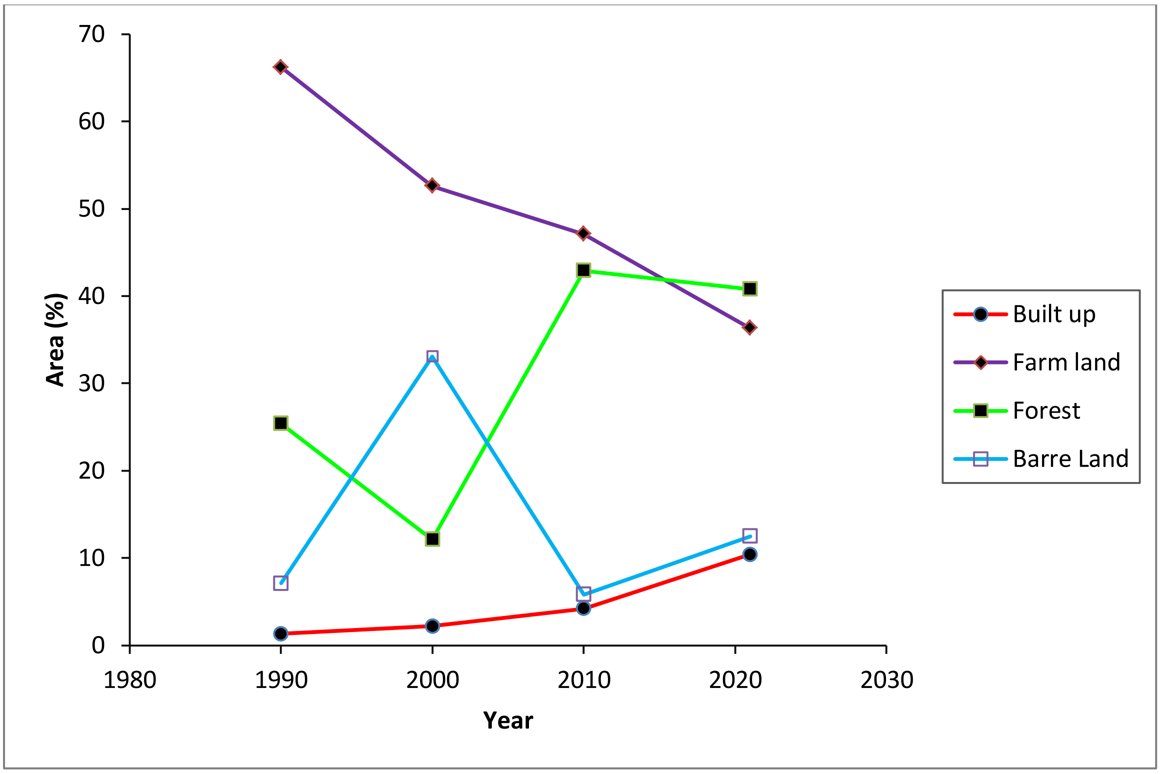

Figure 4.1: LULC percentage of Assosa city from 1990 to 2021

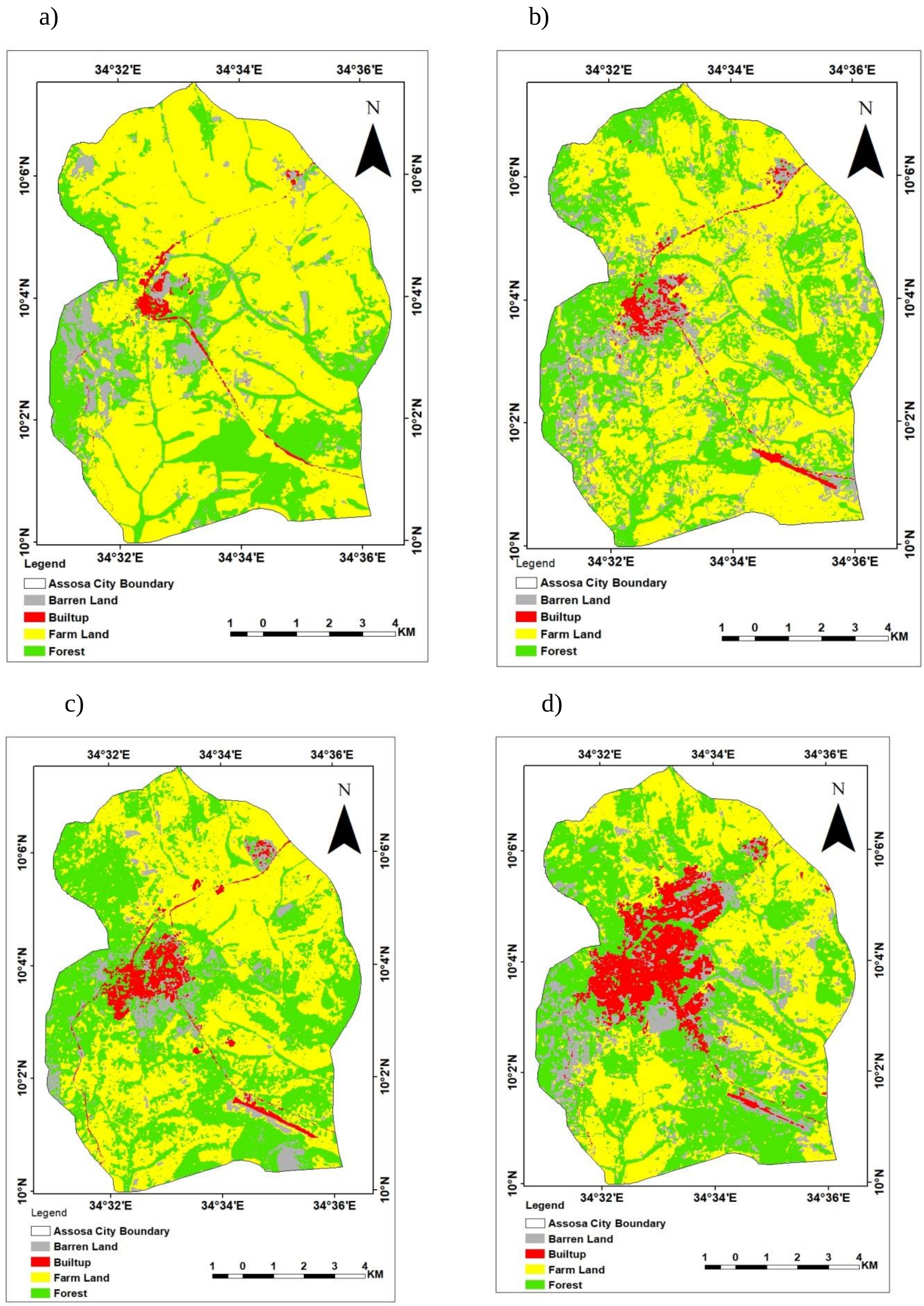

Figure 4.2: LULC maps of Assosa city administration: in 1990(a), 2000(b), 2010 (c) and 2021(d).

4.2 Accuracy assessment

LULC classification accuracy was assessed quantitatively using an error matrix which is the commonly used method in LULC classification accuracy assessment (Chughtai et al., 2021). The classified LULC map of Assosa city in 1990 has an overall classification accuracy of 94%, and a K of 0.93. For the year 2000, the classified LULC image has overall accuracy of 87% and a K of 0.84. Similarly, the classified map of 2010 and 2021 has an overall accuracy of 92% and 93% and K of 0.90 and 0.90 respectively. This implies that all classifications are in the acceptable range because an overall accuracy of each year is greater than 85% and the kappa coefficient greater than 0.80 represents strong (almost perfect) agreement (Rwanga and Ndambuki, 2017) is an indicator for a strong accuracy. The Overall classification accuracy, percentage of user accuracy, producer accuracy, and kappa coefficient (k) are shown in Table 4.2, Table 4.3, Table 4.4, and Table 4.5 for the years 1990, 2000, 2010, and 2021 respectively.

Table 4.2 Error matrix for 1990

LULC type	Built up	Farm land	Forest	Barren	Raw Total	UAC (%)
Built up	20	0	1	1	22	90.90
Farm land	0	87	1	2	89	97.75
Forest	0	2	69	1	73	94.52
Barren land	2	2	0	60	64	93.75
column total	22	89	71	64	246	
PAC	90.90	97.75	97.18	93.75		
Overall accuracy = 94 %			kappa coefficient (k)=0.93			

Note: PAC = Producer Accuracy and UAC = User Accuracy

Table 4.3 Error matrix for 2000

LULC type	Built-up	Farm land	Forest	Barren	Row total	UAC (%)
Built up	32	1	2	3	38	84.21
Farm land	1	38	3	0	42	90.48
Forest	0	4	36	0	40	90.00
Barren Land	0	2	3	33	39	84.62
Column Total	33	45	44	36	158	
PAC	96.97	84.44	80.00	91.67		

Overall accuracy = 87%	kappa coefficient (k)= 0.84

Table 4.4 Error matrix for 2010

LULC type	Built up	Farm land	Forest	Barren land	Raw Total	UAC (%)
Built up	60	3	0	4	67	88.24
Farm land	0	68	1	1	70	97.14
Forest	1	7	100	2	110	90.91
Barren land	1	6	0	113	120	94.17
column Total	63	84	101	120	368	
PAC	95.24	80.95	99.01	94.17		
Overall accuracy = 92% kappa coefficient (k)= 0.90						

Table 4.5 Error matrix for 2021

LULC type	Built up	Farm land	Forest	Barren land	Raw Total	UAC (%)
Built up	79	0	0	3	83	95.18
Farm land	0	10	1	2	12	83.33
Forest	2	1	72	1	76	94.74
Barren land	1	1	4	67	73	91.78
column total	82	12	77	73	244	
PAC	96.34	83.33	93.51	90.54		
Overall accuracy = 93 %			kappa coefficient (k)= 0.90			

4.3 Dynamics of Land use Land cover

Land-use/land-cover patterns in the study area have indicated a significant change between 1990 and 2021.In 1990 farmland and forest covers the largest area (7062.61ha and 2707.14 ha respectively). Whereas barren land and built-up the covers least area (759.10 ha and 138.84ha respectively). In 2021 farmland, forest, barren land and built up area have a coverage of 3874.33 ha, 4349.63 ha, 1335.24 ha and 1108.49 ha respectively.

From 1990 to 2000 coverage of built-up area slightly increased by 98 ha and barren land was significantly increased 2765.26 ha. However, the farm land and forest were decreased by 1447.01 ha and 1416.35ha respectively. From 2000 to 2010 the built up area and forest land increased with 199.24 ha and 3287.37 ha respectively. Within this 10 year, the farmland shows slight reduction (558.86 ha) and the barren land significantly decreased with 2897.59

ha. From 2010 to 2021 Coverage of Built up and barren land area was increased by 672.41ha and 708.47 ha respectively, While farmland and forest significantly decreased by 1152.41ha and 228.53 ha respectively. The change from 1990 to 2021 showed that significant increase of 969.65ha of built-up and 1642.49ha of forest area. Similarly barren land was increased by 576.14 ha. Specifically, farmland was substantially decreased by 3188.28 ha of land within three decades.

In general, over the past three decades, farm land of study areas were in continuous decline, while barren land and forest showed a varying pattern. Conversely to this, built-up areas were continuous increment over the past 30 years. From 2000 to 2010 the forest increment will surprise us but the Causes of forest increment is due the local farmers of the area were planting Eucaliptus Tree (bahirzaf) and Mango on their farm land. This is because of the areas are going to be less fertile and getting money from Eucaliptus tree and mango is Viable than the farmed product. Similarly the increment of built up area is due to population increment over time. The details of LULC change is shown in table 4.6.

Table 4.6 land use land cover change of Assosa city from 1990 to 2021

LULC class		Area (ha)		
	1990-2000	2000-2010	2010-2021	1990-2021
Built-up	98.00	199.24	672.41	969.65
Farm land	-1447.01	-588.86	-1152.41	-3188.28
Forest	-1416.35	3287.37	-228.53	1642.49
Barren land	2765.26	-2897.59	708.47	576.14

4.4 Dynamics of Urban Landscape Patterns

The classification of the multi-temporal satellite images into different class(section 4.1) for the four different time periods of 1990, 2000, 2010 & 2021 has resulted in a highly simplified and abstracted representation of the study area (See figure 4.1). These maps show a clear pattern of increased urban expansion extending both from urban center to adjoining non-built up areas along major transportation corridors. Post classification comparison of the classified images revealed the growth pattern of the city in different directions, the infilling of the open spaces between already built-up areas and the dynamics of urban expansion in the study area. However, it is important to assist the findings with statistical evidences as it is useful to describe the spatial extent and the different patterns of urban growths that have been occurring in the study area. This will help understand how the city is changing over time and to compare the various growth patterns taking place in different time periods quantitatively.

Spatial metrics are powerful tools to quantitatively describe and compare multi-date thematic maps. Five frequently used spatial metrics are selected based on literature review (refer section 3.6) for analysis of built-up area dynamics over space and time at landscape level. The metrics are used to describe the trends and changing patterns of the actual built-up land extracted from classified images. Detail discussion on metrics can be found on section 3.6 of this thesis. All metrics are computed only for the built up area. The outputs presented in table 4.7 were generated for the selected metrics in the form of numeric values for the entire study area from 1990 to 2021 in FRAGSTATS 4.2 software.

Table 4.7 spatial metrics values of built-up area of Asossa city administration in 1990 to 2021.

Year	**Metrics**				
	NP	PD	ED	LPI	FRAC_AM
1990	500	0.5153	1.7315	0.0632	1.1019
2000	1820	1.7077	11.2709	0.8428	1.2240
2010	1890	1.7718	17.3017	2.6973	1.2759
2021	4100	2.3548	22.1669	9.1248	1.2775

The result presented in table 4.7 shows that the continuous rise of number of patches (NP) has led to and is revealed by the rapid urban growth process in the study area landscape throughout the study periods. In 1990 the NP in the region was 500 and rapidly increased to 1820 in 2000 and gradually increased to 1800 in 2010(table 4.7). This could be an indication of fragmented and heterogeneous process of urban growth taking place in the study area. During the 2010 to 2021 period, there was a significant change observed in NP. The peak occurred in 2021 indicating the continuing development of scattered and fragmented urban patches in the study area. This situation can be attributed to a development of small and irregular built up patches around the periphery of the city and in per-urban regions. This could happen as the city expands outward in the form of scattered development, the gap between the per-urban regions and the urban core will decrease by increasing the attractiveness of the per-urban area for development.

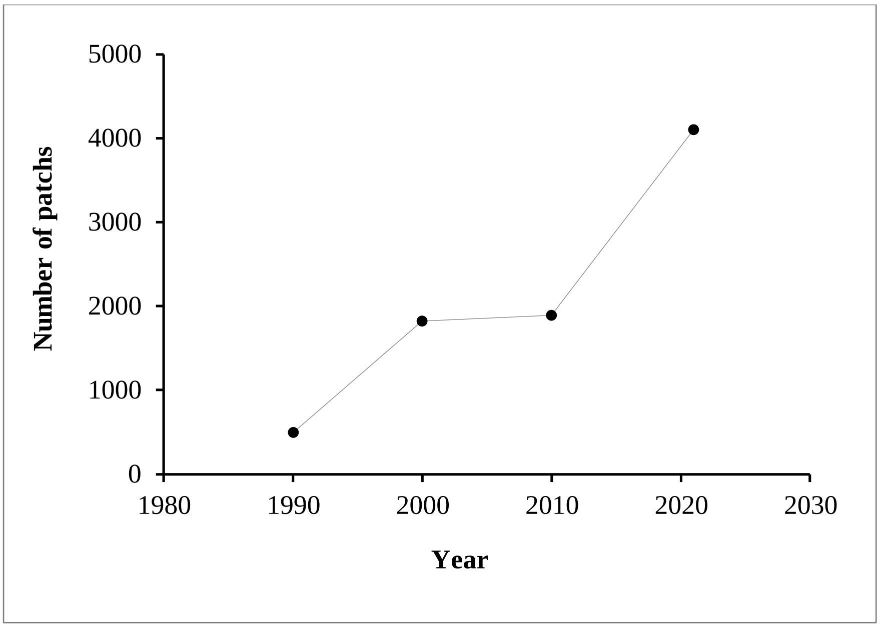

Figure 4.3: Number of built-up patches in Asossa city administration from 1990 to 2021

Similar to NP the patch density (PD) continuously increased throughout the study period. This means the number of new patches in the study area is significantly increased. The PD in 2000 and 2010 are almost similar, which is 1.71 and 1.77 respectively. This indicates that newly forming patches within the two years is less in number. In other words, similar patch density means that some patches located in close proximity to the city Centre are merging with urban core to form a homogeneous urban fabric. But number of patches density is significantly increased in 2021 (figure 4.4).

The increase of PD often leads to increased edge density (ED), as it creates new edge segments in the patch. The result of this study revealed that the edge density (ED) increased from 1.7315 in 1990 to 11.27 in 2000 and17.30 to 21.12 in 2010 to 2021 (Figure 4.4). This shows that there has been significant urban growth with the emergence of various fragmented urban patches observed in the study landscape.

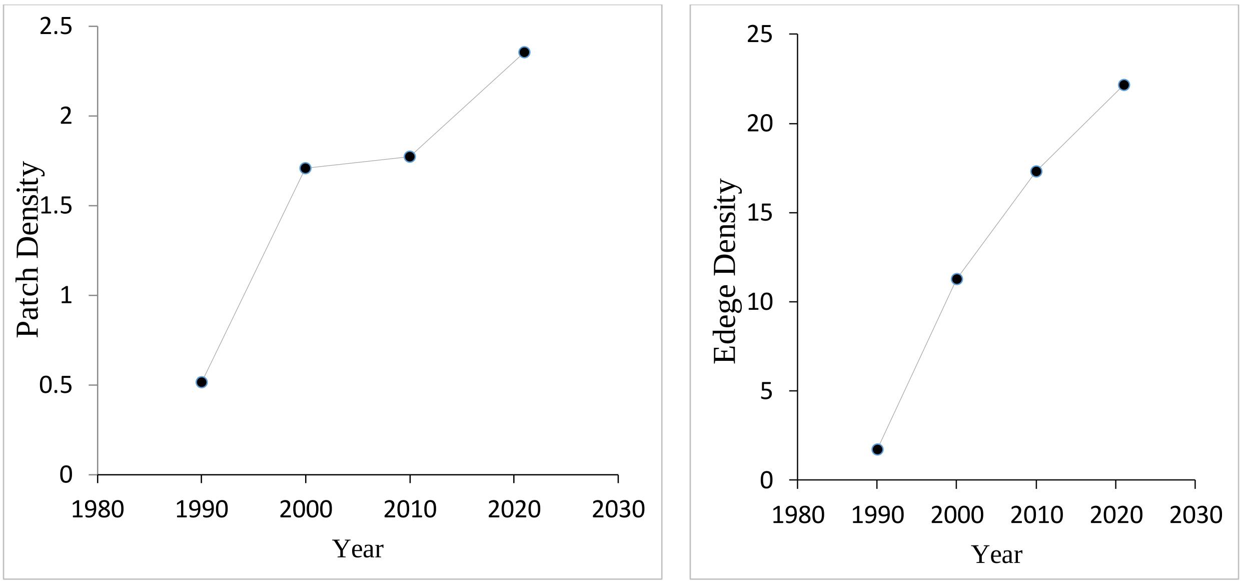

Figure 4.4: patch density (PD) and edge density (ED) of built-up patches in Asossa city administration from 1990 to 2021.

Inherently, the dominant or largest patch in the landscape, which is supposed to be the urban core, is growing over time (Jun et al., 2009). Visual comparison of the classified images confirms the development of urban core in the form of infill and edge expansion (see figure4.1). The gradual expansion of the urban core might have changed the city in to urban agglomeration. This could be one reason for the scattering and fragmented development of the city as urban agglomeration may push development away from the already established urban areas.

The area weighted mean patch fractal dimension (FRAC_AM) is the measure of urban patch shape complexity which describes how patch perimeter increases per unit increase in patch area. In this study, AWMPFD with a consistent increasing trend observed in figure 4.5 shows the complexity and growing irregularity of urban patches due to fragmentation. This can be associated with the partial integration of existing individual patches and probably the formation of fewer new patches during the study periods.

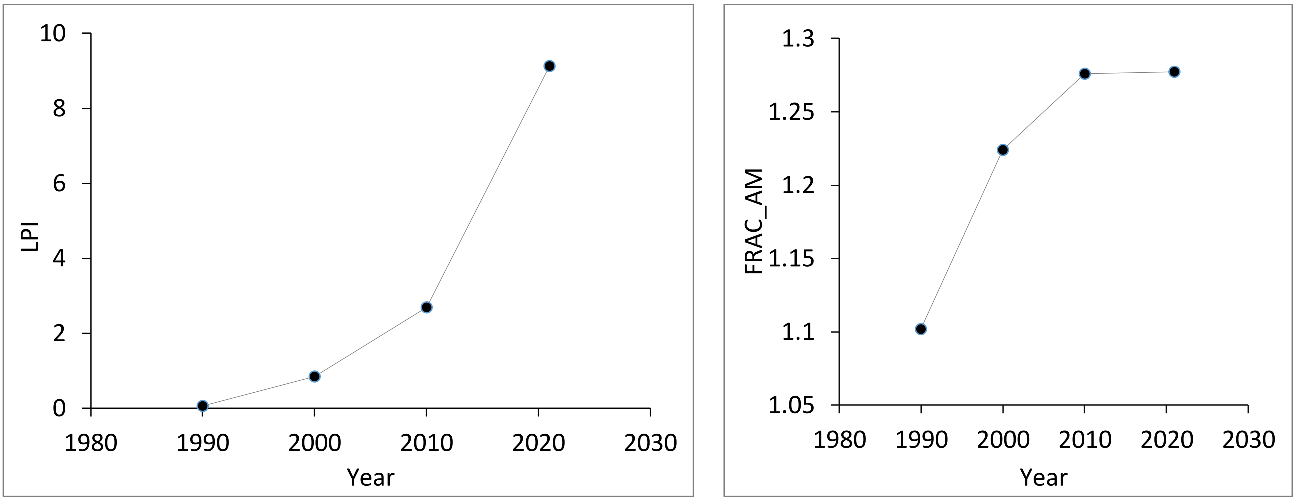

Figure 4.5: largest patch index (LPI) and area weighted mean patch fractal dimension (FRAC_AM) of built-up patches in Asossa city administration from 1990 to 2021

4.5 Forms of urban growth

From the results of spatial metrics analysis of built up area, it has been possible to quantify the trends and patterns of urban dynamics at the city level using the selected metrics. Accordingly, the results of all metrics showed increasing trend throughout the study period. Generally, the spatio-temporal analysis of spatial metrics over the entire study area here described indicates that the urbanization has substantially changed the land cover of the study area, with a significant land conversion. Built up area has been undergoing fragmented development process in all study periods, with substantial increase of built up area during the first and the last period of urbanization, 1990-2000 and 2010-2021.this may be an indicator of urban sprawl. In addition to urban sprawl, which can be witnessed from the substantial increase in number of patches over time, patch density and the largest patch index also revealed that the city is experiencing infill and edge expansion around the urban core (refer figure 4.4). The result of fractal dimension analysis also showed the increasing patch shape complexity of the study area.

4.6 Urban Growth Model

SLEUTH model requires that all input data must be in the same extent, (30x30), same projection and same resolution. All the input layers were resampled to 120, 60, and 30m resolutions corresponding to the coarse, fine, and final calibration using a nearest neighbor algorithm. Finally, the input dataset has been converted to unsigned 8-bit gray scale GIF format.

4.6.1 Slope layer

The slope layer was derived from a United States Geological Survey (USGS) 30m resolution Digital Elevation Model (DEM). The DEM was clipped to the project extent. Slope values were calculated in percent using the ArcGIS Spatial Analyst extension. The resulting image was then converted to an 8 bit GIF image. Figure 4.6 shows slope layer of the study area.

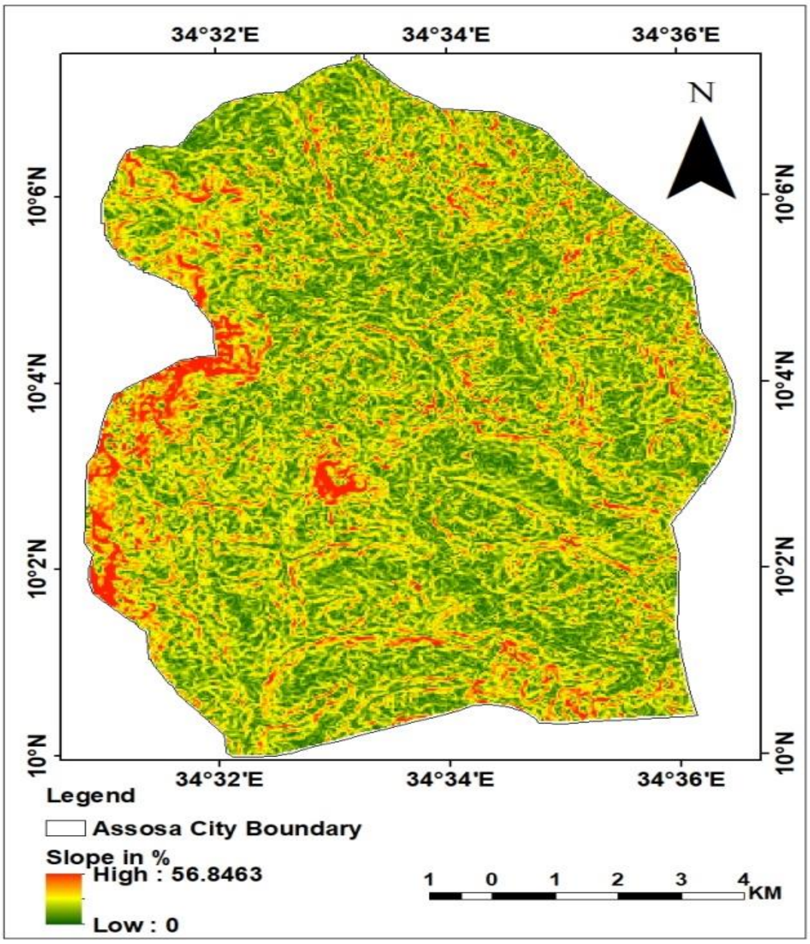

Figure 4.6: slope layer of the study area.

4.6.2 Land use/land cover layers

Land cover data is optional and only required if land use is included in the model. For this study, I examined four classes of land cover change (forest, Built-up area, Farm land and barren land). Land use, land cover type of the Assosa city was prepared from 30 meter resolutions of Landsat satellite images for the following years were obtained:1990 ,2000 ,2010and 2021 by using support vector machine of supervised classification. Figure 4.7 shows land use land cover of the study area.

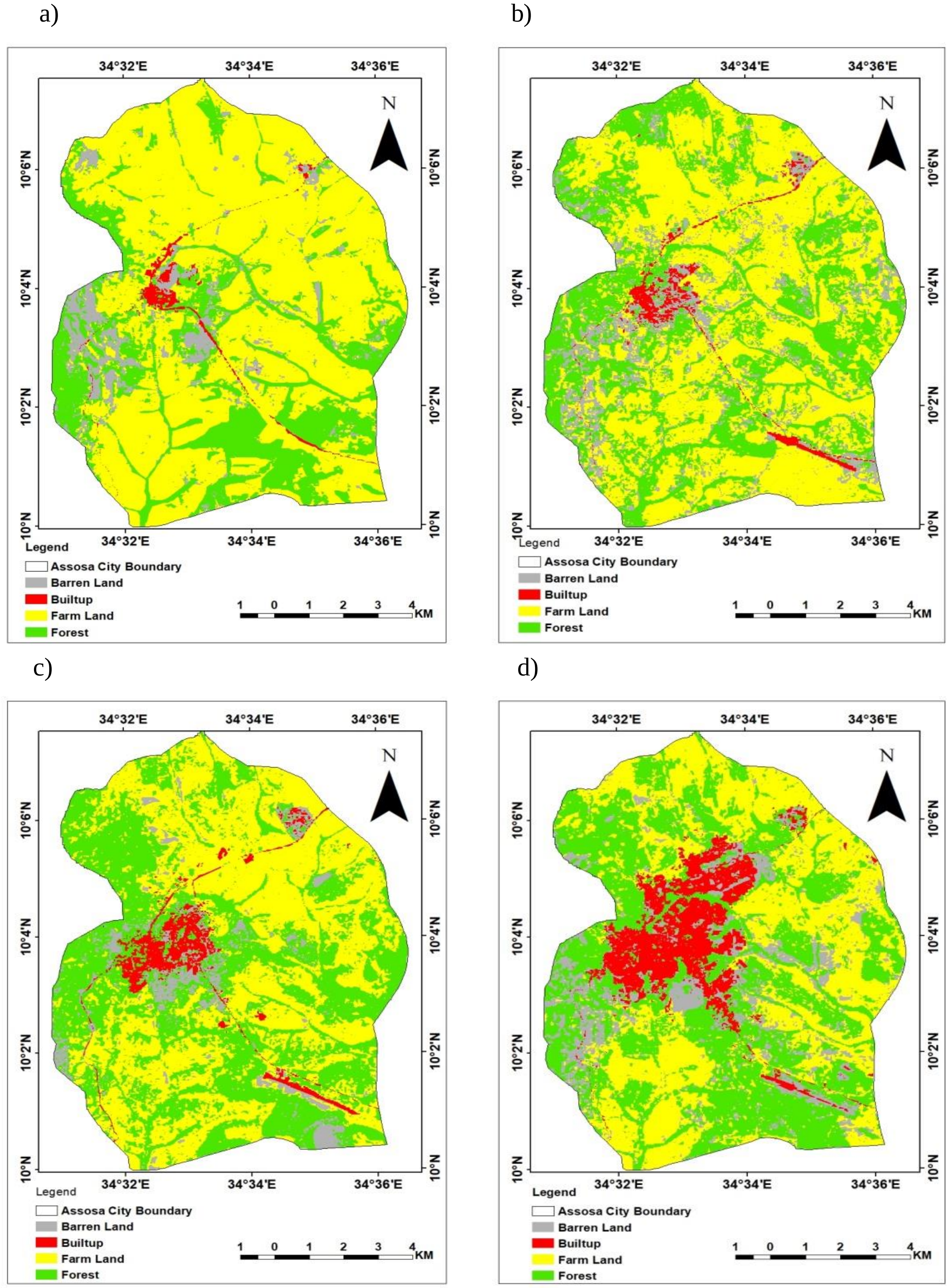

Figure 4.7: land use land cover layers of Assosa city administration in 1990(a), 2000(b), 2010(c) and 2021(d).

4.6.3 Urban Extent

The urban extent for the start year, or seed, is used to initialize the model and is the basis for the CA driven urban growth. For calibration, the earliest urban year is used as the seed, and subsequent urban layers, or control years, are used to measure several statistical best fit values. For this reason, at least four urban layers are needed for calibration: one for initialization and three additional for a least-squares calculation. The definition of "urban extent" is up to the creators of the data set. The model simply requires a binary classification of urban/nonurban (Hua, et al, 2014).

Urban extent layers were extracted from the classified LU/LC layers. Urban extent at the beginning year (known as the "seed") is used to initialize the model, and other years (called a control layer) are applied during calibration phases for the least squares calculation to generate the optimal statistic result.

The urban extent layer only requires a binary classification of urban and non-urban pixels. The pixel values for the layer ranges from 0 to 255 with 0 being non-urban areas and the rest of the non-zero values being defined as urban areas This input provides information on the urbanized area for a given location and serves as a reference for the calibration of the model and a basis on which the goodness of fit of the model is determined. (Chaudhuri & Clarke, 2013). The generated urban extent layer based on land use land cover classification data werw indicated in figure 4.8.

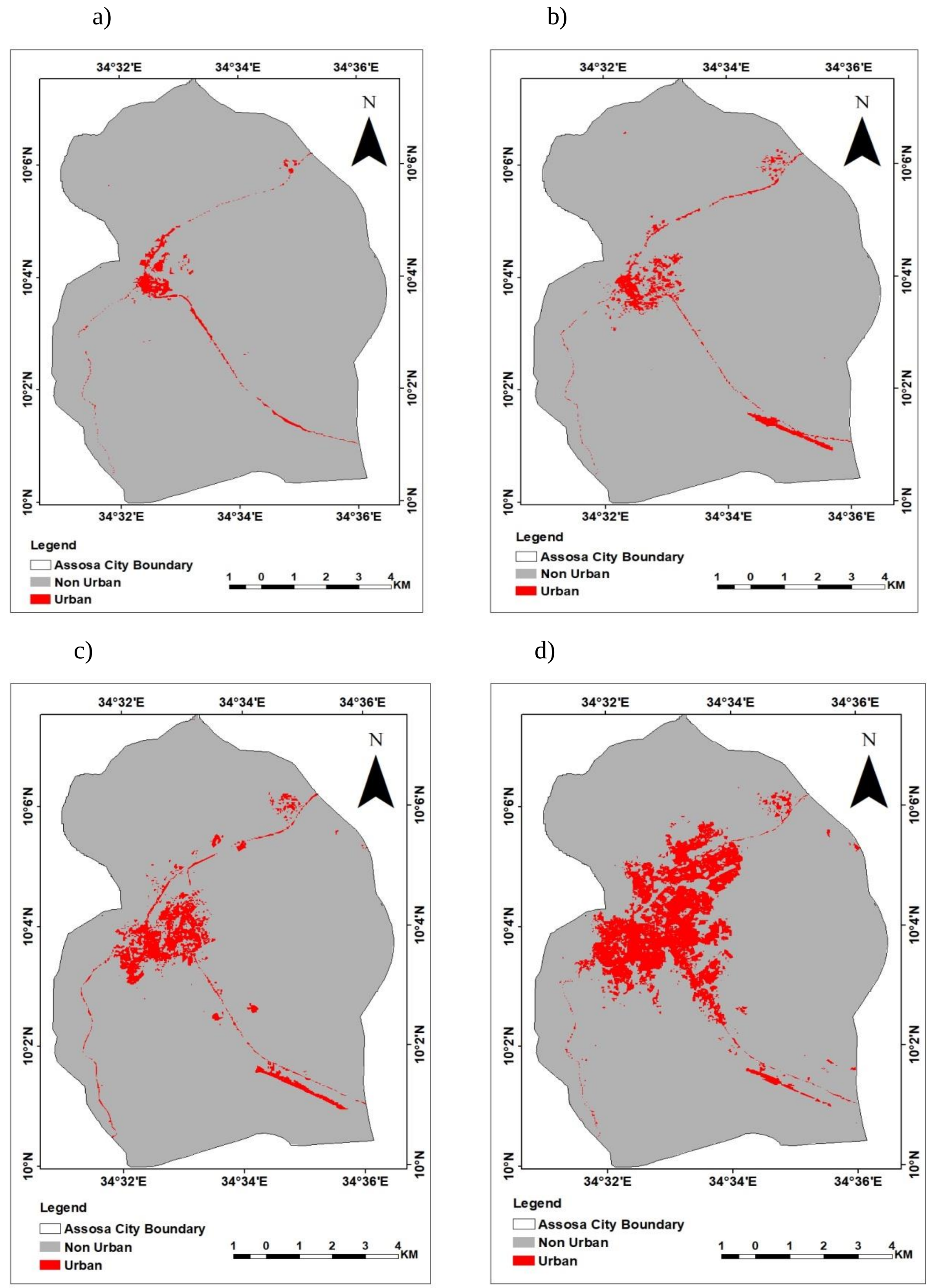

Figure4.8: urban extent of Assosa city Administration in 1990 (a), 2000 (b), 2010 (c) and 2021(d).

4.6.4 Excluded layer

The excluded image defines all locations that are resistant to urbanization. Areas where urban development is prohibited are, like National Parks, Military parks, monuments and water bodies like rivers, Green Areas, /Reserved Areas, Recreation and Environmental Sensitive Area, water canals and dams. In This study, restricted areas are like Cemetery, Light industry, Airport station, Military parks, Electric substation and Environmental Sensitive Area like Urban forest and Green areas. Figure 4.9 Shows excluded are for business as usual (a) planed growth (b) and environment protecting scenarios (c).

a)

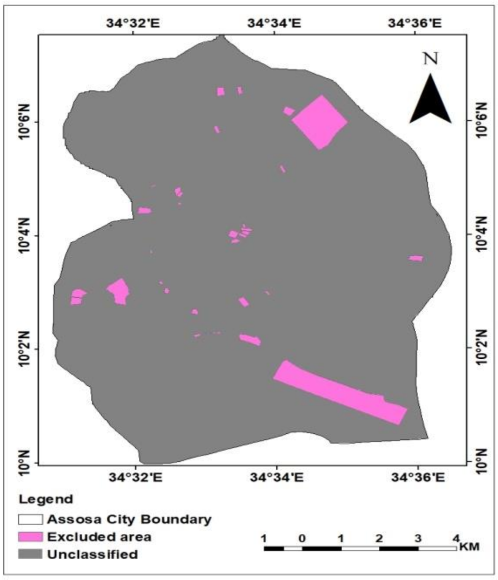

b)

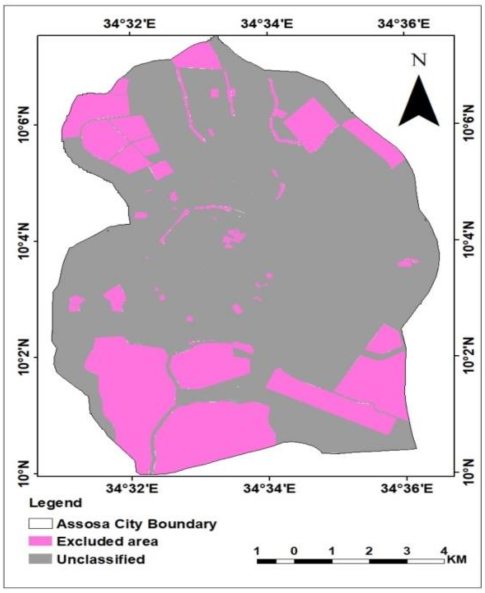

c)

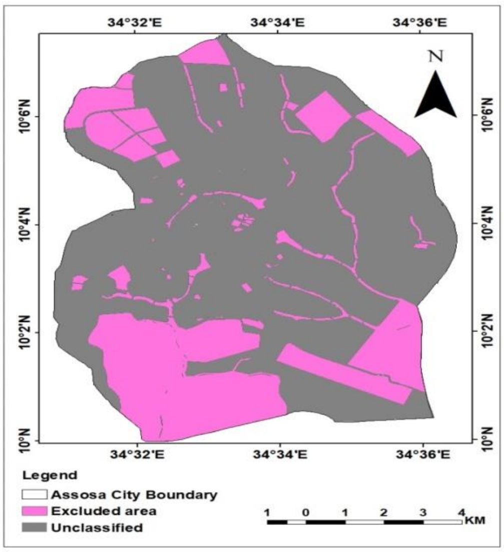

Figure 4.9: excluded layer of the study area

4.6.5 Transportation layer

The inclusion of transportation layers is essential for accurate calibration of the model as transport networks are greatly influential for the manner in which a region develops. As indicated by the data presented in Fig. 4.8, Major road networks have a great influence on the urban growth as cities tend to develop from the downtown to the directions along the transportation system. Road networks for the years 1990, 2000, 2010 and 2021 were digitized from the Landsat image using ArcGIS. After digitization process, all the vector layers were converted into raster format.

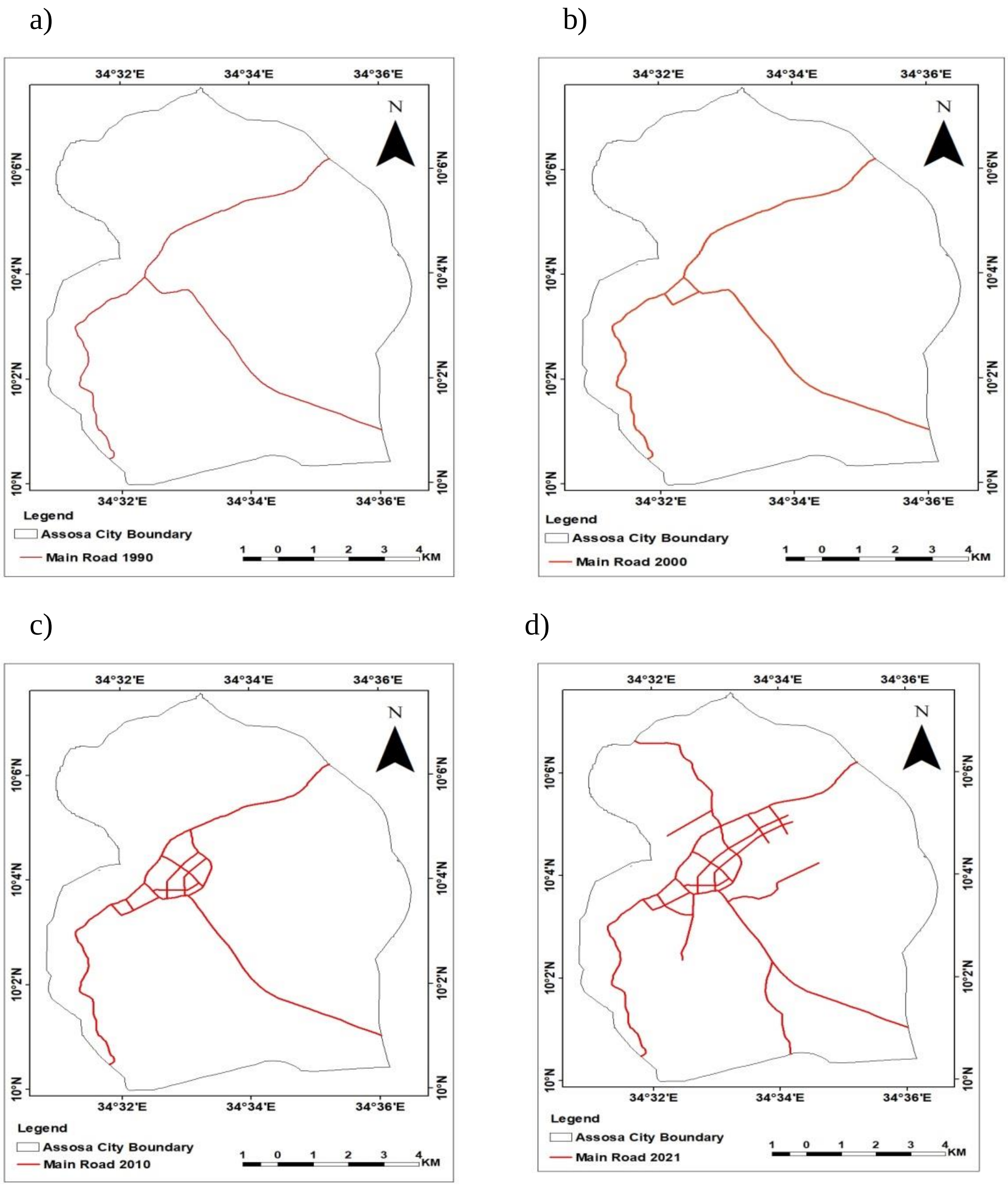

Figure 4.10 Road networks of Assosa city in 1990 (a) 2000(b) 2010(c) and 2021(d)

4.6.6 Hill shade layer

The hill shade layer, only used for visualization purposes, was derived from the same USGS DEM as the slope layer. It can aid in the interpretation of results by providing spatial and topographic context to the urban extent data (Clarke, 2004). By default, shadow and light are shades of gray associated with integers from 0 to 255 (increasing from black to white).The Hill shade layers used for a better spatial visualization rather than participating in the simulation, a shadow in the output image as background. See Figure.4.11.

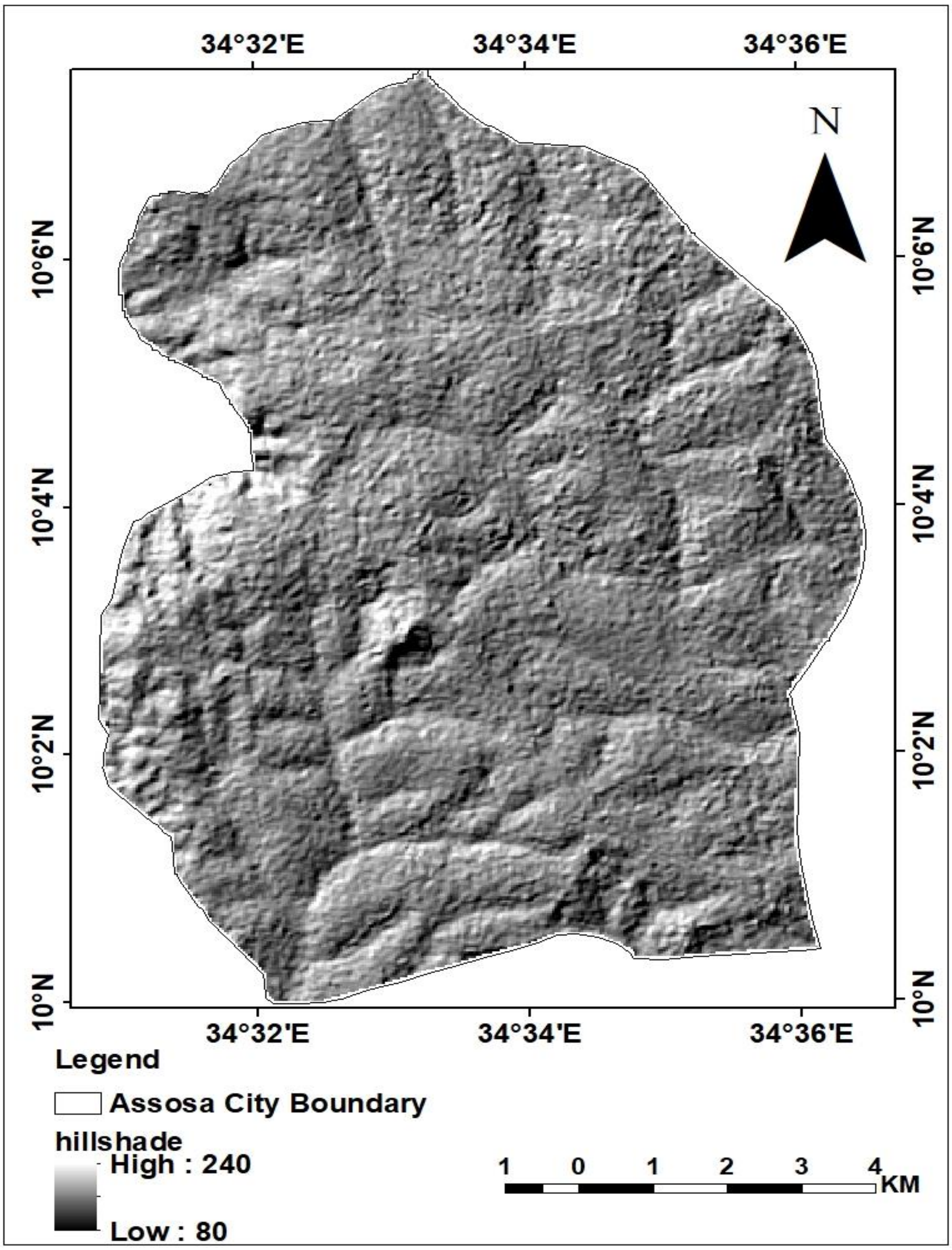

Figure 10.11: hill shade of Assosa City Administration.

4.7 SLEUTH Model Calibration

According to Qi, (2012) the most noteworthy advantage of SLEUTH is that the model has an ability to calculate the optimal combination of coefficients based on the characteristics of the study area. There are five factors to manage the behavior of SLEUTH. This factors are Diffusion, Breed, Spread, Slope Resistance, and Road Gravity, they all varies from 0 to 100. Determining the probability of a random pixel to be urbanized, diffusion controls the entire depressiveness of detached urban cells generated by Spontaneous Growth. In Road Influenced Growth, diffusion specifies the pixel number and interval moving along the road network. A breed constraint influences the New Spreading Center Growth and Road Gravity Growth by controlling the probability to become another growth center of a new born urbanized pixel, and the times of a cell moving along a road in the Road influenced growth. Spread is invoked by the Edge Growth, if there is a sprawl center with more than two urban neighbors in its 3x3 surroundings; spread decides the urbanized probability of other cells in the cluster. The likelihood of settlement extending up steeper slopes is controlled by Slope Resistance.

Before urban growth prediction, a particularly demanding step Calibration is accomplished by the comparison of simulated urbanization with historical growth to refine the controlling coefficients to the specific study area (Dietzel and Clarke, 2007; Akın et al., 2014).

There are two methods available to carry out the calibration phase i.e. Brute force and Genetic Algorithm. As compared to genetic algorithm calibration, brute force calibration is a well-defined, documented and researched method. In this study brute force calibration method has been adopted to sequentially narrow down the ranges of coefficient values with respect to the increasing spatial resolution of input datasets in the three phase i.e., Coarse, fine, final. Accordingly, all the input layers were resampled to 120, 60, and 30m resolutions corresponding to the coarse, fine, and final resolutions, respectively, and exported as unsigned 8-bit, gray scale GIF format images using ArcGIS 10.8. In this study, it was decided to use Lee Sallee metric, which is a measure of spatial fit between the modeled urban growths of the known urban extent of control years, as a primary measure to narrow down the coefficients (K. C. Clarke, 2008).

The Lee-Sallee metric is defined as the “ratio of the intersection and the union of the simulated and actual urban areas, it measures the degree of match between the growth predicted by the model with the actual extent of urban growth that has been seen in the control years (Chaudhuri & Clarke, 2014). This index is comparable in interpretation to the r-square value used in statistics, with a range from 0 to 1 and 1 being a perfect fit using either a single metric or a combination of multiple metrics as the best option to determine a robust goodness of fit has been a controversial subject. When using a combination of the thirteen metrics, there have been a number of metrics that appear to be correlated with each other, leading to a bias in the best fit result. Subsequently, omissions of certain metrics for the analysis have led to a low goodness of fit results (Chaudhuri & Clarke, 2013c).

Coefficients are modified by using the Lee-Sallee metric. As the model runs from the start year of the historical period of 1990 to the end year of the historical period of 2021, the Lee-Sallee metric is calculated for the number of iterations specified. As the model is running through the various years the Lee Sallee metric describes the spatial union between the historical input urban data and the model simulated urban data (Dietzel et al. 2006). Values closer to 1 is a perfect fit between the models simulated image of urban area and the historical image of urban area. Values closer to 0 indicated that the model prediction is unmatched to the historical image.

For the coarse calibration, the data inputs are resampled to a resolution of 120 meters. Within the scenario file the START, STOP, and STEP values are 0, 100, and 25. The amount of Monte Carlo iterations was designated as 4. The output file that is used for calibration is the file control_stats.log. The file is opened in Excel and it is sorted in ascending order by the Lee Sallee metric column. The first five rows of this file are seen in appendix 5 (this procedure is same for fine and final calibrations).

The values of interest are the five initial coefficient values: Diffusion, breed , spread coefficient, slope, and road gravity coefficient. To choose the coefficients that will then be used for the fine calibration, the lowest values of the coefficient will be set to the START value of the coefficient of the fine calibration scenario file and the highest values of the coefficient across the top five runs will be set to STOP value of the coefficient of the fine calibration scenario file. The STEP value increments between the START and STOP value 4-6 times. If only one coefficient value is shown for a certain coefficient as seen through dispersion, START, STOP, and STEP values are chosen that will explore the coefficient values around the one value. Table 4.9 shows the Start, Stop, and Step values chosen for the fine calibration.

Table 4.9 Coefficient range chosen for fine calibration.

Coefficient	Start	Step	Stop
Diffusion	0	5	20
Bread	25	50	75
Spread	50	60	75
Slope	25	50	100
Road gravity	1	5	25

Fine calibration is used to further narrow down the range of the coefficients and step interval of 1-3 units between the lowest and the highest predicted coefficients is used to determine the Final value for the calibration. Each phase of the calibration produce thirteen goodness of fit metrics of the current run as similar to coarse calibration above. For the fine calibration, the data inputs are resampled to a resolution of 60 meters.

Table 4.10 Coefficient range chosen for final calibration

Coefficient	Start	Step	Stop
Diffusion	1	1	5
Bread	22	1	27
Spread	45	1	50
Slope	22	1	27
Road gravity	11	1	21

For the final calibration, data at a 30 meter resolution is used. The scenario file is modified using the coefficient ranges obtained from the fine calibration. This mode is used for forecasting the future urban growth of the study area. Again the control_stats.log file is sorted in descending order from the Lee Sallee metrics. After sorting, the coefficient values from the top Lee Sallee metric are chosen as both the START and STOP values. The step values are assigned to be one (Table 4.11).

Table 4.11 Coefficient ranges chosen for the Forecast Coefficient Run.

Coefficient	Start	Step	Stop
Diffusion	1	1	1
Bread	23	1	23
Spread	50	1	50
Slope	22	1	22
Road gravity	13	1	13

For the prediction run, the STOP values from the best calibrated coefficients (derived from the coarse, fine, and final calibration) are needed. In order to do this, the SLEUTH model is run again (using the 30m resolution data) for the historical time period, using the coefficients from the final calibration. The scenario file is modified using the coefficient ranges obtained from the final calibration. In order to get the coefficient values for the prediction mode of this model, the avg.log file is used. The avg.log file is seen in Table4.12

Table 4.12 Selected Forecast Coefficient Run values.

year	index	diffusion	spread	breed	Slope resistance	Road gravity
2000	1	1.09	54.68	25.15	19.35	13.26
2010	2	1.21	60.41	27.79	15.22	13.68
2021	3	1.35	67.39	31	9	14.34

For the stop year of the historic data, 2021, the diffusion, breed, spread, slope resistance, and road gravity values are obtained. This are then rounded to the nearest whole number. These coefficient values which will be used for the prediction mode are seen in Table 4.13.

Table 4.13: Coefficients chosen for prediction mode.

Coefficient	Values
Diffusion	2
Bread	67
spread	31
Slope resistance	9
Road gravity	14

4.8 Spatiotemporal urban growth Simulation

The growth of urban areas was analyzed with respect to its coverage inside the boundary of Assosa city administration during the year 1990, 2000, 2010 and 2021. Temporal variation in the Landsat series of satellites based on urban classification reveals substantial changes in urban areas. The study indicates that changes of urban area from 138.84 ha in 1990 to 1108.49 ha in -2021. As indicated in table 4.14, the percentage of the built-up growth area was increasing more than 50 percent within a decade. Growth rate of Built-up area during 1990 to 2000 was 138.84 ha to 236.84 ha, which is a change of 70.6 % and 2000 to 2010 the change of built up area was 236.84 ha to 436.84 ha, which is 84.1 % change within 10 year. From the year 2010 to 2021 the growth of built-up area increased significantly from 436.08 ha to 1108.49 ha (152.2 %). The built-up growth rate for the consecutive study period is listed in table 4.14.

Table 4.14 Areal extents, percentage change and growth rate over time of urban area in Assosa city from 1990 to 2021

year	Area (ha)	Change (ha)	Change (%)	Growth rate /year
1990	138.84			
2000	236.84	98.00	70.6	7.06
2010	436.08	199.24	84.1	8.41
2021	1108.49	672.41	154.2	14.02

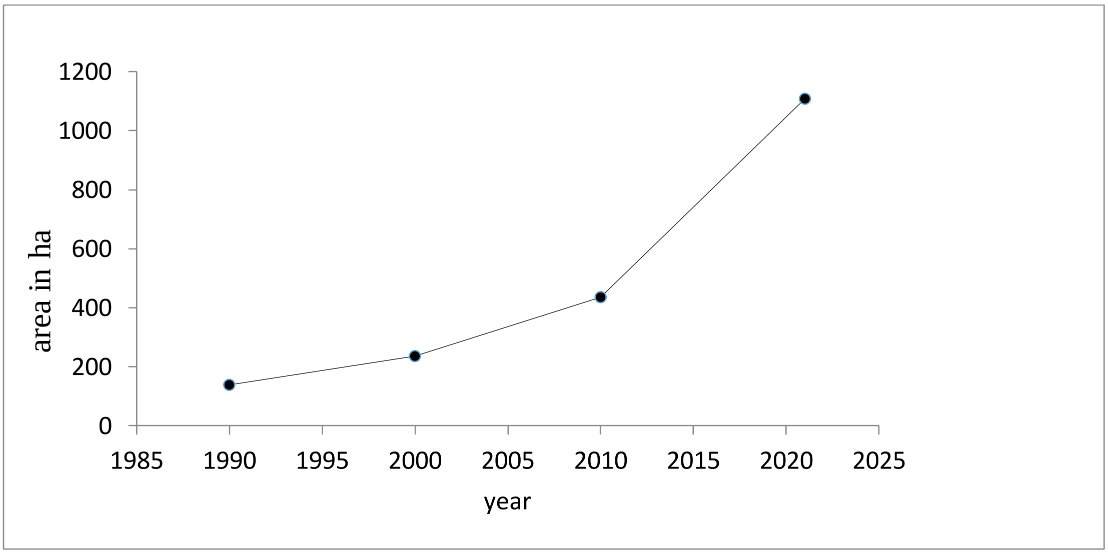

Figure 4.12 Urban built-up area of Assosa City during 1990–2021

The urban extent in the study area grew rapidly from 1990 to 2021 (Fig. 4.12). During this years, the urban expansion primarily involved sprawling and infilling (new growth occurring through infilling of free spaces within the developed area) growth at the urban edges. The rapid urban growth primarily occurred in the centers and edges of the new urban areas (for more, see section 4.3).

4.9 Future Urban Growth Predication

As a computer simulation model, SLEUTH can generate various alternative future urban growth patterns, supporting the exploration of diverse what-if policy scenarios. This can be achieved mainly through two options: changing parameter values and/or data inputs. The change of parameter values such as growth coefficients and self-modification parameters affects the growth rules and rates and results in alternative future growth. This option can also be used to assume the impact of certain growth types on overall growth systems. Numerous alternative scenarios are possible with this option, but the practical meanings are clear when extreme changes in model parameters are taken into account. Incremental changes in model parameters will only give abstract meaning to alternative future growth. Another way is using different input data sets. This option is rather to assume different initial conditions and to see how the future is affected by this. Different levels of initial cell values can be assigned to the desired reference layers such as exclusion and transportation, or new elements can be added. Depending on what to include or exclude, this can be a more vivid option to address the change of certain policy directions for a given study area. SLEUTH does not use socio economic data and it only uses geographic data of the built environment. Thus the design of possible scenarios is limited to this. Different conditions can be considered only in a physical sense.

This study has designed three growth scenarios based on the second option: business as usual, planned growth and Environment-protecting scenarios. The main difference between them is on the data used for exclusion layer. For those scenarios the result shows different urban growth extent (see table 4.15).

4.9.1 Urban growth Predication by Business as usual scenario

In this growth scenario, existing urban areas are expected to expand simply based on the previous growth pattern. It is based on its own developmental process. The quantitative demand for land use is mainly based on the urban change from 1990 to 2021, and the SLEUTH Model is used to predict the land use change in 2030, 2040 and 2050. For this scenario only existing exclusions like Cemetery, Light industry, Electric substation and Airport are taken as exclusion for future urban development. In 2030 the predicted result of business as usual scenario shows that 1801.75 ha of land will be covered by Built up area. Similarly With increasing trends, in 2040 (2493.33 ha) and 2050 (3267.35ha) Assosa city will be covered by built up area.

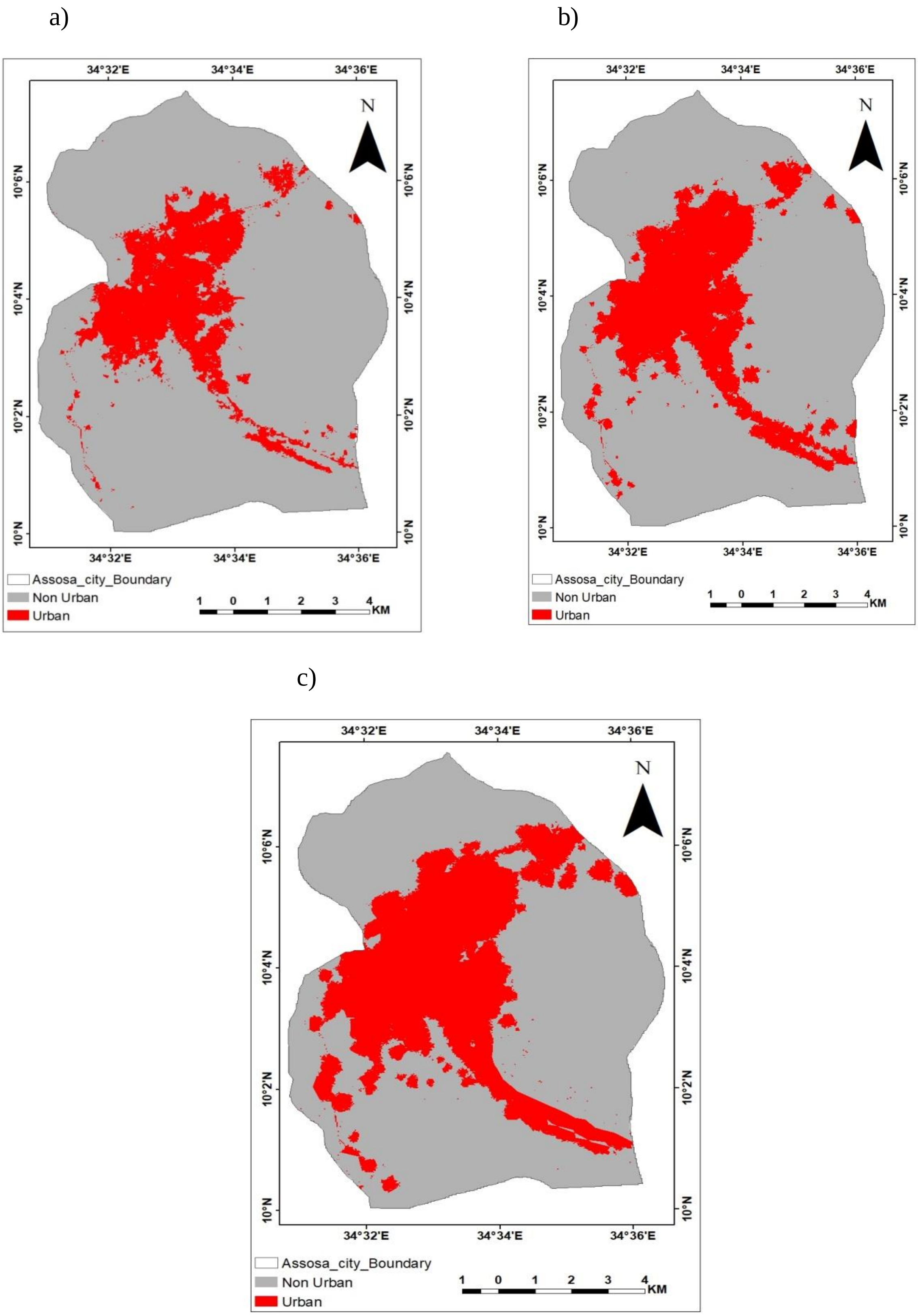

Figure 4.13 Predicted Map of Assosa City Administration in 2030(a), 2040(b) and 2050(c) Under Business as usual scenario.

4.9.2 Urban growth Predication by Planned growth scenario

The planned growth scenario reflects a stronger commitment to spatially focused growth and resource protection .In addition to exclusion layers considered in the first scenario, open space, rural agriculture and all growth restricted areas as indicated by the newly developed structural plan (2021) of Assosa city are taken as growth restricted areas .Under this scenario, urban growth is well protected and limited according to the city structural plan. The results shows that, the built up area will be 1723.79 ha in 2030 and 2207.75 ha in 2040. Similarly in 2050 the area covered by built up will be 2885.7ha. This result is less than 380 ha compared to the first scenarios. This means if the urban growth of the study area continues as planned scenario, 380 ha of land will be conserved in 2050 and natural resource also may not been depleted.

a) b)

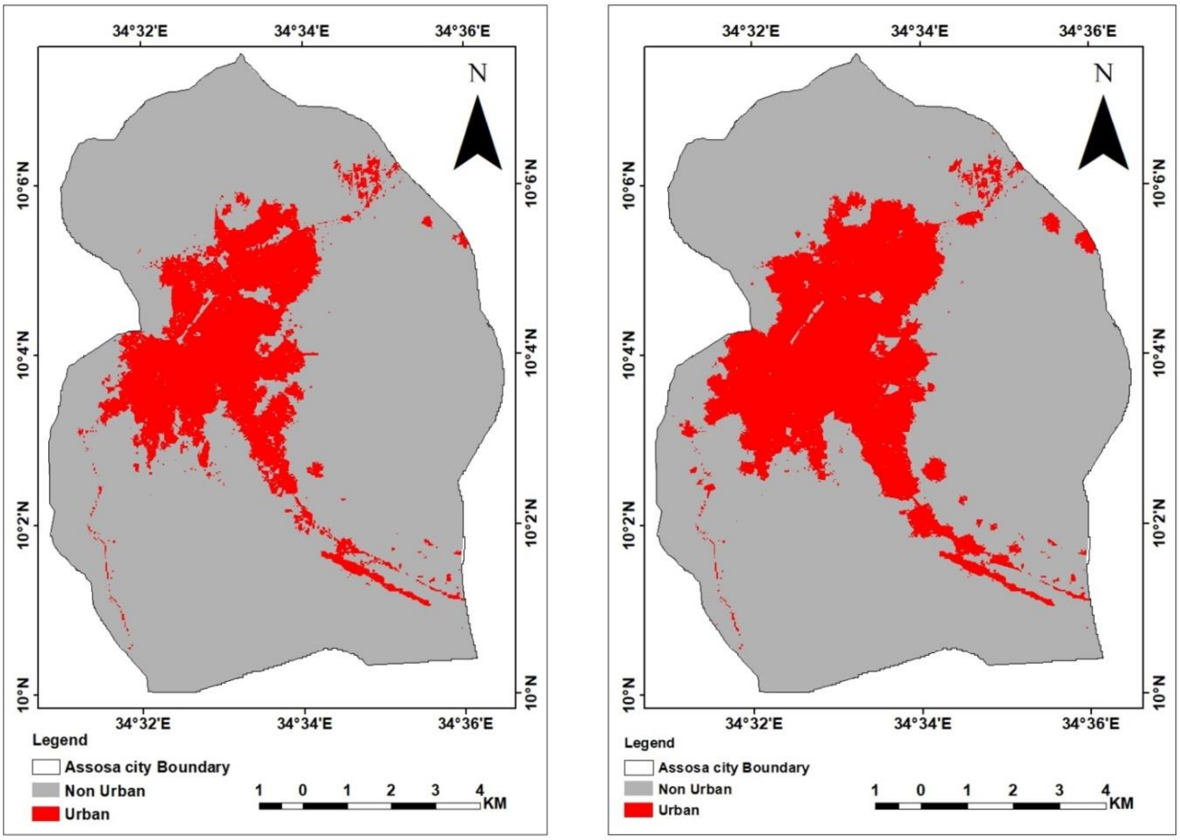

Figure 4.14 Predicted Map of Assosa City Administration in 2030 and 2040 under planned growth scenario.

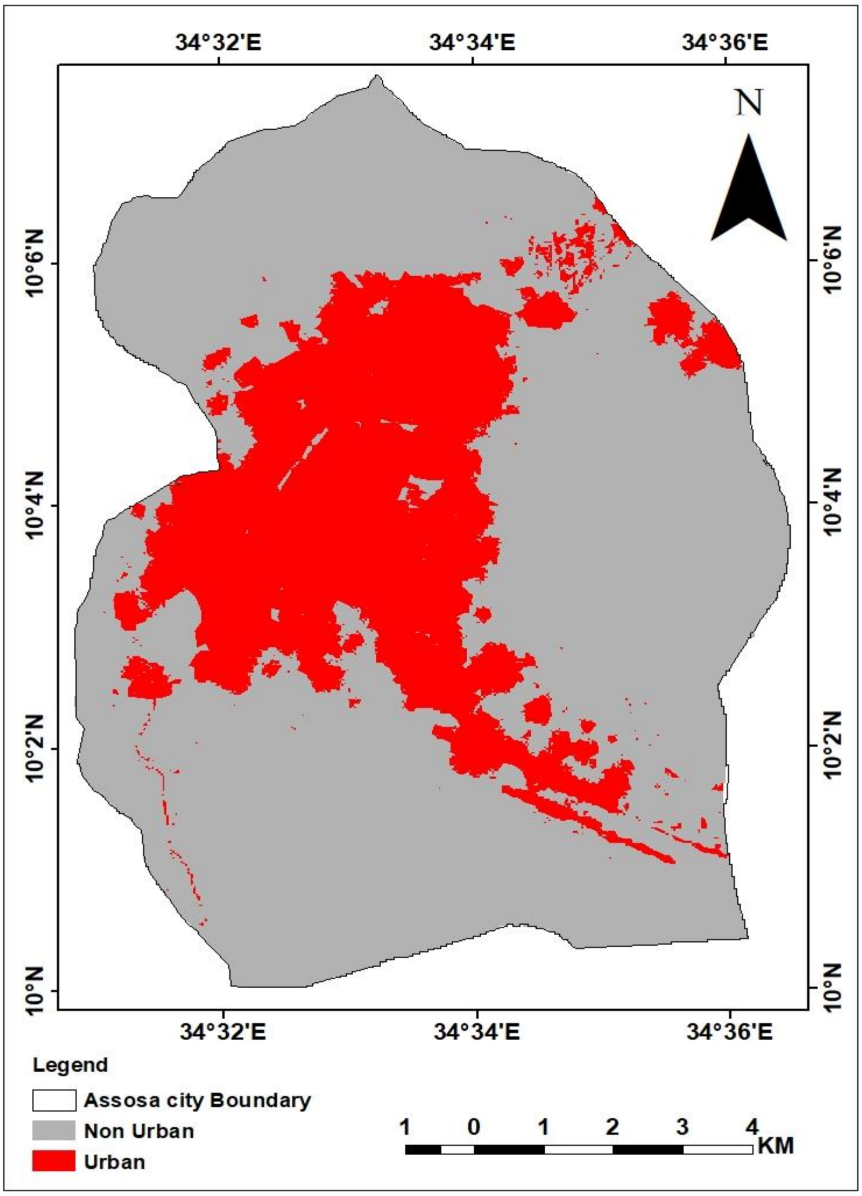

Figure 4.15 Predicted Map of Assosa City Administration in 2050 under planned growth scenario.

4.9.3 Urban growth Predication by Environment-protecting scenario

Environment-protecting scenario reflects a more strict set of policies targeted toward limited growth and natural resource protection .The data elements for the excluded layer are similar to those in the planned growth case, but additionally, urban forest, water streams are highly considered. Environment-protecting scenario, a slow-growth scenario gives emphasis to natural conservation and ecosystem protections. The disadvantage of this scenario is it hinders urban growth .The results of this scenario prediction show that 1718.08 hectare of land will be covered by built up area in 2030. Similarly in 2040 and 2050 the built up area will reach 2179.9ha and 2778.62 ha respectively. The result of the year 2050 is less than 488.73 ha as compared to Business as usual and 107.08 ha as compared to planed growth scenarios. This indicates that more land and more natural resources will be conserved. The natural environment and the ecosystem will be not affected if this scenario is applied for the future urban development but on conversely the urban growth will be slowed. So, to use the available allowed land for urbanization, strict rule and regulation is necessary. Figure 4.16 and 4.7 shows the predicted result of Environment-protecting scenarios. The statistical results are shown in table 4.15 and figure 4.18.

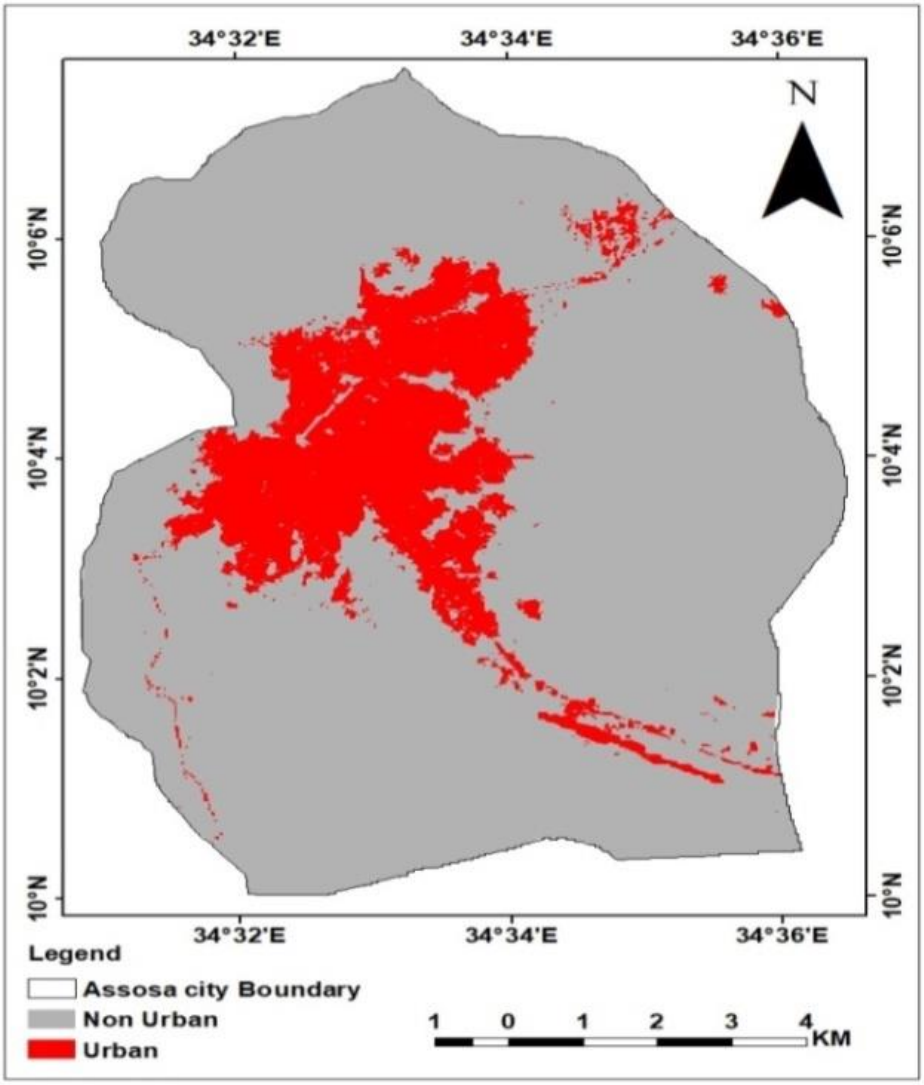

Figure 4.16: Predicted Map of Assosa city Administration in 2030 Under Environment-protecting scenario.

a) b)

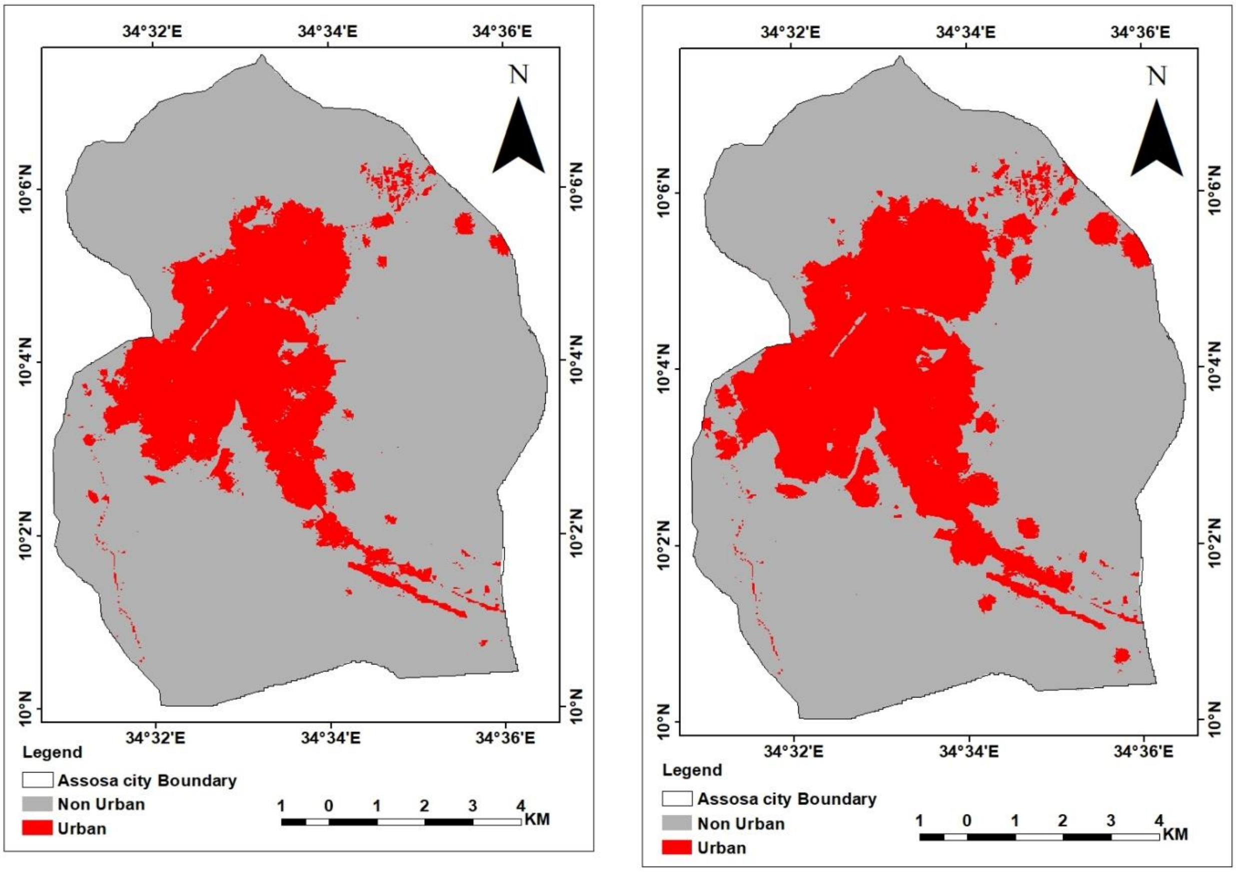

Figure 4.17: Predicted Map of Assosa City Administration in 2040 (a) and 2050(b) under Environment-protecting scenario.

Table 4.15: Predicted built-up area of Asossa city administration under three scenarios from 2030 to 2050.

Scenarios	2030	2040	2050
	Area (ha)	Area (ha)	Area (ha)
Business as usual scenario	1801.75	2493.33	3267.35
Planned growth scenario	1723.79	2207.75	2885.7
Environment-protecting scenario	1718.08	2179.9	2778.62

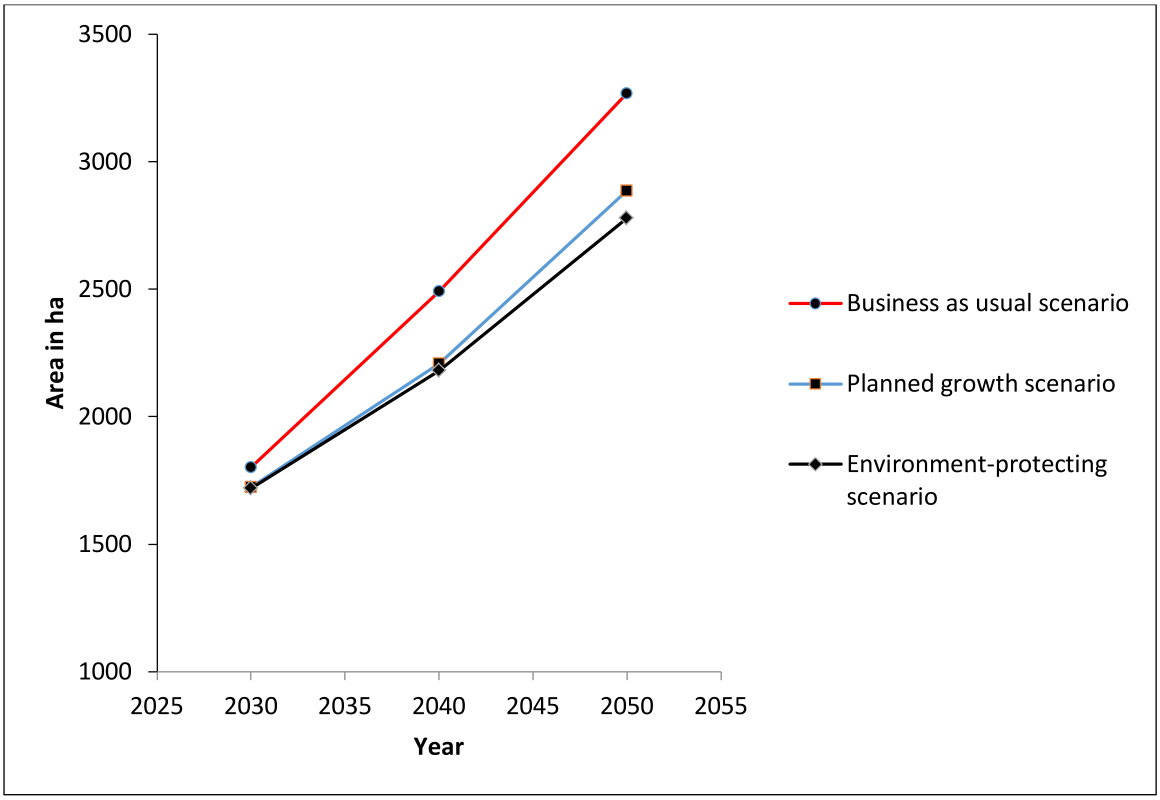

Figure 4.18: predicted builtup area in 2030, 2040 and 2050 of Assosa city adminstraation.

CHAPTER FIVE: CONCLUSION AND RECOMMENDATION

5.1 Conclusion

Urban growth is being increasingly challenging in an era of rapid urbanization and intensive human activity. It is important to understand the physical processes in urban systems to plan for long-term sustainable development of cities. To simulate the future scenarios, SLEUTH modeling serves as a diagnosis for the urban development in Assosa city.

This study was aimed to model the urban spatial growth of Assosa city using the SLEUTH mode. The LULC maps were produced for the years 1990, 2000, 2010, and 2021 with high accuracy. Based on the classified map of the study area between 1990 and 2021; the coverage of built-up areas was increased rapidly. While the coverage of Farm land significantly decreased. The Forest and barren land were showed varying pattern.

This study has also made it possible to successfully understand the change happened on the urban growth pattern at landscape urban level. Assosa city experienced fragmented urban growth process, particularly, at the fringe areas with substantial built up increase while, the core of the city underwent relatively compact growth by infilling open spaces and through edge expansion over time. The built up area in the metropolis has grown from 138.84 ha in 1990 to 1108.49 ha in 2021. The rate of growth per year was 7.1% from1990-2000 and 8.4% from 2000-2010. From 2010-2021 the growth rate of built-up area was 14.0% per annually. In total, 970 ha of non-built up has been converted to urban area within 3 decades. Analyzing the spatial extent and rate of urban growth as well as identifying the growth directions alone does not give sufficient insight in to the patterns of urban growth processes, which are important to have a better understanding of the urban growth pattern. To bridge this gap, landscape metrics are used. five metrics namely: number of patches (NP), patch density (PD), edge density (ED), largest patch index (LPI) and area weighted mean patch fractal dimension (AWMPFD) were utilized to evaluate the patterns of urban growth and processes experienced in Assosa city at landscape level. Based on the number of patches (NP), the built up area experienced fragmented growth process all throughout study periods , with the second period of urbanization (2000 to 2010) witnessing slight increase of built up area and substantial increase of built up area in the first and the last decades. The patch density and largest patch index also shown that the city is experiencing infill and edge expansion around the urban core. The area weighted mean patch fractal dimension (AWMPFD) showed increasing trends.

This indicates that the entire built up area will keep on getting more complex and hence, fragmented over time mainly at the fringe areas.

This research applied the SLEUTH model to predict the future urban growth scenarios of Assosa city for the next coming 30 years. The model was validated based on urban pattern 1990 to 2021 and used to predict the scenarios in 2030, 2040 and 2050. Three scenarios were considered; Business as Usual, planned and environment-protecting scenarios. Using Business as Usual scenarios, built-up area was predicted as 1801.75 ha (in 2030), 2493.33 ha (in 2040) and 3267.35 ha for the year 2050. Planned and environment-protecting scenario, predicted the lowest urban growth rate. In planned growth scenario, urban area for the year 2030, 2040 and 2050 was predicted as 1723.79 ha, 2207.75 ha and 2885.7 ha respectively. With environment-protecting scenario the predicted values of urban built-up area was 1718.08 ha (in 2030), 2179.9 ha (in 2040) and2778.62 ha (in 2050). Planned and environment-protecting scenarios are preferable in terms of sustainability and urban planning policy could play more attention to environmental protection and restoration and put more emphasis on the harmony between human and nature. These scenarios are helpful for decision makers who are exploring various sustainable urban development options before making any plan formulation. Therefore findings of this study provide useful insights into the characteristics of urban development and formulating urban development plans.

5.2 Recommendations

This study was focused on the prediction of future urban growth of Assosa City. Based on the findings of this study, the following recommendations have been drawn.

- Since the value of information extracted from landscape metrics is dependent on the quality of image classification, future studies could attempt to improve on the classification accuracy of the satellite images utilized in this study. This could help in solving the issues involved with image consistency.
- This study used 10 years gap urban historical data to predict the future growth. However, currently urbanization is growing rapidly and shows variation even within a year. Future studies should inspect within a short period of time for example within 5 year and less.
- This study considered only the historical spatial variables of the study area. With respect to scenario simulation, SLEUTH models are rather limited to the variables directly considered by the model. Thus, it may also be disputable and subject to further research if more sophisticated means on urban simulation (like socio-economic and demographic variables) may be implementable.
- Currently, the study model is limited to predict only Urban built-up. However, there are of course other land-use to be considered and should inspect for future studies.

REFERENCES

AbdEl-Kawy OR, Rød JK , Ismail HA, & Suliman AS (2011). Land use and land cover change detection in the western Nile delta of Egypt using remote sensing data. *Applied geography*, *31*(2), 483-494.

Al-shalabi M, Billa L, Pradhan, B, Mansor S, & Al-Sharif A (2013) .Modelling urban growth evolution and land-use changes using GIS based cellular automata and SLEUTH models: the case of Sana'a metropolitan city, Yemen. *Environmental earth sciences*, *70*(1), 425-437.

Angel S, Parent J, & Civco D (2007) .Urban sprawl metrics: an analysis of global urban expansion using GIS. In *Proceedings of ASPRS 2007 Annual Conference, Tampa, Florida May* (Vol. 7, No. 11). Citeseer.

Angel S, Parent J, Civco DL, Blei, A, & Potere, D (2011). The dimensions of global urban expansion: Estimates and projections for all countries, 2000–2050. *Progress in Planning*, *75*(2), 53-107.

Arsanjani JJ, Helbich M, & Noronha E (2013). Spatiotemporal simulation of urban growth patterns using agent-based modeling: The case of Tehran. *Cities*, *32*, 33-42.

Barow I, Megenta M, & Megento, T (2019). Spatiotemporal analysis of urban expansion using GIS and remote sensing in Jigjiga town of Ethiopia. *Applied Geomatics*, *11*(2), 121-127.

Barredo JI, Kasanko M, McCormick N, & Lavalle C (2003). Modelling dynamic spatial processes: simulation of urban future scenarios through cellular automata. *Landscape and urban planning*, *64*(3), 145-160.

Bekalo MT (2009). *Spatial metrics and Landsat data for urban landuse change detection: case of Addis Ababa, Ethiopia* (Doctoral dissertation).

Benayas JR, Martins A, Nicolau JM & Schulz, JJ (2007). Abandonment of agricultural land: an overview of drivers and consequences. *CAB reviews: Perspectives in agriculture, veterinary science, nutrition and natural resources*, *2*(57), 1-14.

BerlingWolff S, & Wu J (2004) Modeling urban landscape dynamics: a case study in Phoenix, USA. *Urban ecosystems*, *7*(3), 215-240.

Bhatta B (2010). *Analysis of urban growth and sprawl from remote sensing data*. Springer Science & Business Media.

Bhatta B, Saraswati S, & Bandyopadhyay D (2010). Urban sprawl measurement from remote sensing data. *Applied geography*, *30*(4), 731-740.

Braimoh AK & Onishi T (2007). Spatial determinants of urban land use change in Lagos, Nigeria. *Land use policy*, *24*(2), 502-515.

Chaudhuri G,& Clarke, K (2013).The SLEUTH land use change model: A review. *Environmental Resources Research*, *1*(1), 88-105.

Chaudhuri G, & Clarke K. (2014). Temporal accuracy in urban growth forecasting: A study using the SLEUTH model. *Transactions in GIS*, *18*(2), 302-320.

Chen Y, Li X., Zheng Y, Guan Y, & Liu X. (2011). Estimating the relationship between urban forms and energy consumption: A case study in the Pearl River Delta, 2005–2008. *Landscape and urban planning*, *102*(1), 33-42.

Chughtai AH, Abbasi H, & Karas IR (2021). A review on change detection method and accuracy assessment for land use land cover. *Remote Sensing Applications: Society and Environment*, *22*, 100482.

Crosbie RS, Pickett T, Mpelasoka FS, Hodgson G, Charles S P & Barron OV (2013). An assessment of the climate change impacts on groundwater recharge at a continental scale using a probabilistic approach with an ensemble of GCMs. *Climatic Change*, *117*(1), 41-53.

Desa, UN. (2017). Population division *World Population Prospects*

Dewan AM & Yamaguchi Y (2009). Land use and land cover change in Greater Dhaka, Bangladesh: Using remote sensing to promote sustainable urbanization. *Applied geography*, *29*(3), 390-401.

DeWind J & Holdaway J (2005). Internal and international migration in economic development. In *Fourth Coordination Meeting on International Migration, United Nations, New York* (pp. 26-27).

Dieleman F & Wegener M (2004). Compact city and urban sprawl. *Built environment*, *30*(4), 308-323.

Dietzel C & Clarke, KC (2007). Toward optimal calibration of the SLEUTH land use change model. *Transactions in GIS*, *11*(1), 29-45.

Dietzel C, Herold M., Hemphill JJ & Clarke KC (2005). Spatio-temporal dynamics in California's Central Valley: Empirical links to urban theory. *International journal of geographical information science*, *19*(2), 175-195.

Dubovyk O, Sliuzas, R, & Flacke J (2011). Spatio-temporal modelling of informal settlement development in Sancaktepe district, Istanbul, Turkey. *ISPRS Journal of Photogrammetry and Remote Sensing*, *66*(2), 235-246.

Foody GM (2002) Status of land cover classification accuracy assessment. *Remote sensing of environment*, *80*(1), 185-201.

Getu K & Bhat HG (2021). Analysis of spatio-temporal dynamics of urban sprawl and growth pattern using geospatial technologies and landscape metrics in Bahir Dar, Northwest Ethiopia. *Land Use Policy*, *109*, 105676.

Guan D, Li H, Inohae T, Su W, Nagaie T & Hokao K (2011). Modeling urban land use change by the integration of cellular automaton and Markov model. *Ecological modelling*, *222*(20-22), 3761-3772.

Hu Z & Lo CP (2007) .Modeling urban growth in Atlanta using logistic regression. *Computers, environment and urban systems*, *31*(6), 667-688.

Huang Q, Parker DC, Filatova T & Sun S (2014). A review of urban residential choice models using agent-based modeling. *Environment and Planning B: Planning and Design*, *41*(4), 661-689.

Jantz CA, Goetz SJ, & Shelley MK (2004). Using the SLEUTH urban growth model to simulate the impacts of future policy scenarios on urban land use in the Baltimore-Washington metropolitan area. *Environment and Planning B: Planning and Design*, *31*(2), 251-271.

Jenberu, AA., & Admasu TG (2020). Urbanization and land use pattern in Arba Minch town, Ethiopia: driving forces and challenges. *GeoJournal*, *85*(3), 761-778.

Jensen JR (1996). *Introductory digital image processing: a remote sensing perspective* (No. Ed.2). Prentice-Hall Inc..

Ji W, Ma J, Twibell RW, & Underhill K (2006). Characterizing urban sprawl using multi-stage remote sensing images and landscape metrics. *Computers, Environment and Urban Systems*, *30*(6), 861-879.

Jiang L, Deng X., & Seto K (2013). The impact of urban expansion on agricultural land use intensity in China. *Land use policy*, *35*, 33-39.

Kaufmann RK, Seto KC, Schneider A, Liu Z, Zhou L & Wang W (2007). Climate response to rapid urban growth: Evidence of a human-induced precipitation deficit. *Journal of Climate*, *20*(10), 2299-2306.

Lambin EF, Turner BL, Geist HJ, Agbola SB, Angelsen A, Bruce JW, & Xu J (2001). The causes of land-use and land-cover change: moving beyond the myths. *Global environmental change*, *11*(4), 261-269.

Li D, & Bou-Zeid E (2013). Synergistic interactions between urban heat islands and heat waves: The impact in cities is larger than the sum of its parts. *Journal of Applied Meteorology and Climatology*, *52*(9), 2051-2064.

Li X & Yeh AG (2000). Modelling sustainable urban development by the integration of constrained cellular automata and GIS. *International journal of geographical information science*, *14*(2), 131-152.

Liu XI & Lathrop Jr, (2002). Urban change detection based on an artificial neural network. *International Journal of Remote Sensing*, *23*(12), 2513-2518.

Longley PA, & Mesev V (2000).On the measurement and generalisation of urban form. *Environment and planning A*, *32*(3), 473-488.

Lu D, & Weng Q (2007). A survey of image classification methods and techniques for improving classification performance. *International journal of Remote sensing*, *28*(5), 823-870.

Martinuzzi S, Gould WA, & González MR (2007). Land development, land use, and urban sprawl in Puerto Rico integrating remote sensing and population census data. *Landscape and urban planning*, *79*(3-4), 288-297.

McGarigal K (2015). FRAGSTATS help. *University of Massachusetts: Amherst, MA, USA*, *182*.

Mekonnen Y & Hailu A (2020). Modeling Urban Growth and Land Use Transition Using SLEUTH Model: The Case of Dilla City, Ethiopia.

Mertens B, & Lambin EF (2000). Land-cover-change trajectories in southern Cameroon. *Annals of the association of American Geographers*, *90*(3), 467-494.

Miller MD (2012). The impacts of Atlanta's urban sprawl on forest cover and fragmentation. *Applied Geography*, *34*, 171-179.

Newman G, Lee J, & Berke P (2016). Using the land transformation model to forecast vacant land. *Journal of Land Use Science*, *11*(4), 450-475.

Oguz H, Klein AG, & Srinivasan R (2007). Using the SLEUTH urban growth model to simulate the impacts of future policy scenarios on urban land use in the Houston-Galveston-Brazoria CMSA. *Research Journal of Social Sciences*, *2*(1), 72-82.

Overmars KD, De Koning GH. & Veldkamp A (2003). Spatial autocorrelation in multi-scale land use models. *Ecological modelling*, *164*(2-3), 257-270.

Perumal K, & Bhaskaran R (2010). Supervised classification performance of multispectral images. *arXiv preprint arXiv:1002.4046*.

Perveen S, Kamruzzaman M, & Yigitcanlar T (2017). Developing policy scenarios for sustainable urban growth management: A Delphi approach. *Sustainability*, *9*(10), 1787.

Phiri D & Morgenroth J (2017). Developments in Landsat land cover classification methods: A review. *Remote Sensing*, *9*(9), 967.

Poelmans L & Van Rompaey A(2009). Detecting and modelling spatial patterns of urban sprawl in highly fragmented areas: A case study in the Flanders–Brussels region. *Landscape and urban planning*, *93*(1), 10-19.

Pontius Jr, RG, & Schneider LC (2001). Land-cover change model validation by an ROC method for the Ipswich watershed, Massachusetts, USA. *Agriculture, ecosystems & environment*, *85*(1-3), 239-248.

Rafiee R Mahiny AS Khorasani N Darvishsefat AA& Danekar A (2009). Simulating urban growth in Mashad City, Iran through the SLEUTH model (UGM). *Cities*, *26*(1), 19-26.

Rahimi A (2016). A methodological approach to urban land-use change modeling using infill development pattern—a case study in Tabriz, Iran. *Ecological Processes*, *5*(1), 1-15.

Rwanga SS & Ndambuki JM (2017). Accuracy assessment of land use/land cover classification using remote sensing and GIS. *International Journal of Geosciences*, *8*(04), 611.

Sangawongse S (2006). Land-use/land-cover dynamics in Chiang Mai: appraisal from remote sensing, GIS and modeling approaches. *CMU Journal*, *5*(2), 243-254.

Silva EA, & Clarke KC (2005). Complexity, emergence and cellular urban models: lessons learned from applying SLEUTH to two Portuguese metropolitan areas. *European Planning Studies*, *13*(1), 93-115.

Sinha P, Verma NK & Ayele E. (2016). Urban built-up area extraction and change detection of Adama municipal area using time-series Landsat images. *Int. J. Adv. Remote Sens. GIS*, *5*(8), 1886-1895.*nd assessment*, *186*(3), 1765-1780.

Sudhira HS, Ramachandra TV, & Jagadish KS (2004). Urban sprawl: metrics, dynamics and modelling using GIS. *International Journal of Applied Earth Observation and Geoinformation*, *5*(1), 29-39.

Sun H, Forsythe W & Waters N (2007). Modeling urban land use change and urban sprawl: Calgary, Alberta, Canada. *Networks and spatial economics*, *7*(4), 353-376.

Thapa RB, & Murayama Y (2010). Drivers of urban growth in the Kathmandu valley, Nepal: Examining the efficacy of the analytic hierarchy process. *Applied Geography*, *30*(1), 70 83.

Torrens PM. (2011). Calibrating and validating cellular automata models of urbanization. *Urban remote sensing: Monitoring, synthesis and modeling in the urban environment*, 335-345.

Un-Habitat (2012). *State of the World's Cities 2008/9: Harmonious Cities*. Routledge.

Veldkamp A & Verburg PH. (2004). Modelling land use change and environmental impact. *Journal of Environmental Management*, *72*(1-2), 1-3.

Watkiss BM (2008). *The SLEUTH urban growth model as forecasting and decision-making tool* (Doctoral dissertation, Stellenbosch: Stellenbosch University).

Woldegerima T, Yeshitela K & Lindley S (2017). Characterizing the urban environment through urban morphology types (UMTs) mapping and land surface cover analysis: The case of Addis Ababa, Ethiopia. *Urban ecosystems*, *20*(2), 245-263.

Wolfram S (2018). *Cellular automata and complexity: collected papers*. crc Press.

Wondrade N, Dick Ø. B & Tveite H (2014). GIS based mapping of land cover changes utilizing multi-temporal remotely sensed image data in Lake Hawassa Watershed, Ethiopia. *Environmental monitoring and assessment*, *186*(3), 1765-1780.

Yang X, & Lo CP (2003). Modelling urban growth and landscape changes in the Atlanta metropolitan area. *International journal of geographical information science*, *17*(5), 463-488.

Yeh, CT & Huang, SL (2009). Investigating spatiotemporal patterns of landscape diversity in response to urbanization. *Landscape and Urban Planning*, *93*(3-4), 151-162.

Yu XJ, & Ng CN (2007). Spatial and temporal dynamics of urban sprawl along two urban–rural transects: A case study of Guangzhou, China. *Landscape and urban planning*, *79*(1), 96-109.

APPENDICES

Appendix 1 GCP used for validation of the model

station	Easting	Northing	Remark	27	670812.1	1115852	Builtup27
1	669156.9	1111366	Builtup01	28	670793.7	1115573	Builtup28
2	669186.6	1111669	Builtup02	29	670714	1115817	Builtup29
3	669238.4	1111656	Builtup03	30	671547.8	1115246	Builtup30
4	669603.6	1111840	Builtup04	31	671420.8	1115148	Builtup31
5	669535.7	1111826	Builtup05	32	671302.8	1115150	Builtup32
6	669135.7	1111762	Builtup06	33	671580.6	1115048	Builtup33
7	669082.7	1111858	Builtup07	34	671520.3	1115001	Builtup34
8	669247.5	1111797	Builtup08	35	670516.1	1114822	Builtup35
9	669240	1111581	Builtup09	36	670608.5	1114676	Builtup36
10	669420.4	1111907	Builtup10	37	670548.3	1114104	Builtup37
11	669372.7	1111493	Builtup11	38	670569.4	1114141	Builtup36
12	669450.1	1111834	Builtup12	39	670392	1114101	Builtup39
13	669296.4	1111900	Builtup13	40	670301.3	1114068	Builtup40
14	669143.7	1111836	Builtup14	41	670298.8	1113975	Builtup41
15	669175	1111973	Builtup15	42	670330.5	1113926	Builtup42
16	669435.5	1112046	Builtup16	43	670221.6	1113904	Builtup43
17	668659.3	1111561	Builtup17	44	670260.7	1114038	Builtup44
18	668703.7	1112055	Builtup18	45	670353.6	1113962	Builtup45
19	668345.9	1112891	Builtup19	56	670240.2	1113937	Builtup46
20	668253.1	1112835	Builtup20	47	670263.4	1113945	Builtup47
21	668114.5	1112754	Builtup21	48	670185.5	1113944	Builtup48
22	667982.1	1111997	Builtup22	49	670158.8	1113969	Builtup49
23	668106.4	1112625	Builtup23	50	670252.7	1113939	Builtup50
24	668560.8	1111992	Builtup24	51	670208.7	1113990	Builtup51
25	670284.7	1115450	Builtup25	52	670184.7	1114044	Builtup52
26	670576.9	1115585	Builtup26	53	670147.4	1114109	Builtup53
54	670221.1	1114194	Builtup54	73	669885.7	1113751	Builtup73
56	670363.4	1114150	Builtup56	75	669928.9	1113653	Builtup002
57	670344.1	1114165	Builtup57	76	669865.2	1113667	Builtup003

58	670311.6	1114199	Builtup58	77	669848.8	1113649	Builtup004
59	670294.4	1114221	Builtup59	78	669825.5	1113670	Builtup005
60	670277.2	1114230	Builtup60	79	669810.8	1113692	Builtup006
61	670269.4	1114202	Builtup61	80	669801.1	1113707	Builtup007
62	670236.6	1114275	Builtup62	81	672153.9	1114300	Farmland01
63	670165.3	1114225	Builtup63	82	672090.4	1113226	Farmland02
64	670199.4	1114216	Builtup64	83	672855.5	1111917	Farmland04
65	670186.8	1114189	Builtup65	84	672111.4	1111371	Farmland05
66	670201.2	1114164	Builtup66	85	671916.7	1110867	Farmland03
67	670218.2	1114153	Builtup67	86	671770.4	1110631	Farmland06
68	670196.1	1114150	Builtup68	87	671653.4	1110169	Farmland07
69	670170.2	1114101	Builtup69	88	671446.8	1110397	Farmland08
70	670188.1	1114119	Builtup70	89	670172.7	1115876	Farmland09
71	670187.2	1114019	Builtup71	90	671018.5	1116394	Farmland10
72	669920.7	1113694	Builtup72	91	670705.5	1116559	Forest01
93	670799.8	1116458	Forest03	92	671770.4	1110631	Forest02
94	670828.8	1116336	Forest04	111	670500.7	1115789	Forest21
95	670663.2	1115954	Forest05	112	670490.7	1115776	Forest22
96	670680.5	1115995	Forest06	113	670593	1115418	Forest23
97	670664.8	1115982	Forest07	114	670689.6	1115467	Forest24
98	670643.4	1116002	Forest08	115	670580.9	1115399	Forest25
99	670672.2	1115939	Forest09	116	670735.6	1115427	Forest26
100	670693.1	1115923	Forest10	117	670530.9	1115377	Forest27
101	670675.5	1115917	Forest11	118	670868	1115538	Forest28
102	670670	1115888	Forest12	119	670812.4	1115469	Forest29
103	670660	1115889	Forest13	120	670688.7	1115397	Forest30
104	670682.6	1115880	Forest14	121	672142.2	1115029	Forest31
105	670606.7	1115877	Forest15	122	672291.9	1114820	Forest32
106	670637.7	1115907	Forest16	123	671886.5	1114186	Forest33
107	670536.1	1115817	Forest17	124	671675	1113067	Forest34
108	670555.5	1115807	Forest18	125	671706.4	1113135	Forest35
109	670523.5	1115776	Forest19	126	671603	1113168	Forest36
110	670510	1115775	Forest20	127	671628.8	1113122	Forest37
165	668541	1112516	Barren66	184	671423.5	1111903	Barren47

166	668415.2	1112326	Barren65	185	671590.3	1112044	Barren46
167	668307.4	1112134	Barren64	186	671679.4	1111670	Barren45
168	667525	1112526	Barren63	187	671400.7	1112190	Barren44
169	669953.6	1111748	Barren62	188	672020.5	1112446	Barren43
170	670203.7	1111651	Barren61	189	671883.3	1112467	Barren42
171	671230.2	1111180	Barren60	190	672008.7	1112397	Barren41
172	671335.6	1111183	Barren59	191	671736.9	1112419	Barren40
173	671382.1	1111292	Barren58	192	671971	1112908	Barren39
174	671627.2	1111230	Barren57	193	671925.8	1112957	Barren38
175	671722.3	1111191	Barren56	194	671865	1112929	Water37
176	671799.9	1111289	Barren55	195	671723.9	1112971	Barren36
177	671626.9	1111096	Barren54	196	672374.5	1113066	Barren35
178	671630.6	1111612	Barren53	197	672368.7	1113172	Barren34
179	671578.2	1111669	Barren52	198	671618.9	1113784	Barren33
180	671550.7	1111748	Barren51	199	671523.9	1113426	Barren32
181	671519.2	1111830	Barren50	200	671455.1	1113271	Barren31
182	671624.5	1111960	Barren49	216	669440.7	1114225	Barren15
183	671468.3	1111909	Barren48	217	669278.9	1115094	Barren14
202	671356.9	1113009	Barren29	219	670753.7	1114458	Barren12
203	671370.8	1112846	Barren28	220	669038	1115500	Barren11
204	671300.9	1113099	Barren27	221	670009.6	1115652	Barren10
205	671216.9	1112945	Barren26	222	670429.3	1115166	Barren09
206	670180.5	1113438	Barren25	223	668631.1	1114575	Barren08
207	669895.3	1113331	Barren24	224	671014.7	1115412	Wter4
208	670098.5	1113305	Barren23	225	671471.7	1116034	Barren07
209	670290.3	1113243	Barren22	226	671258.9	1115612	Barren06
210	669451.1	1113604	Barren21	227	672082	1115265	Barren05
211	669348.7	1113505	Barren20	228	671708.5	1114838	Barren04
212	669435.2	1113359	Barren19	229	669954.6	1115178	Water3
213	670082	1112912	Barren18	230	670097.8	1114583	Barren03
214	670051.7	1112732	Barren17	231	670648.7	1114006	Barren02
215	670657.6	1113300	Barren16	232	670218.3	1113790	Barren01
234	669996.5	1113639	Barren1	233	670359.4	1113639	Barren1
235	671660.2	1110856	Water1	234	669996.5	1114364	Water2

Appendix 2 LULC classification validation map of the study area

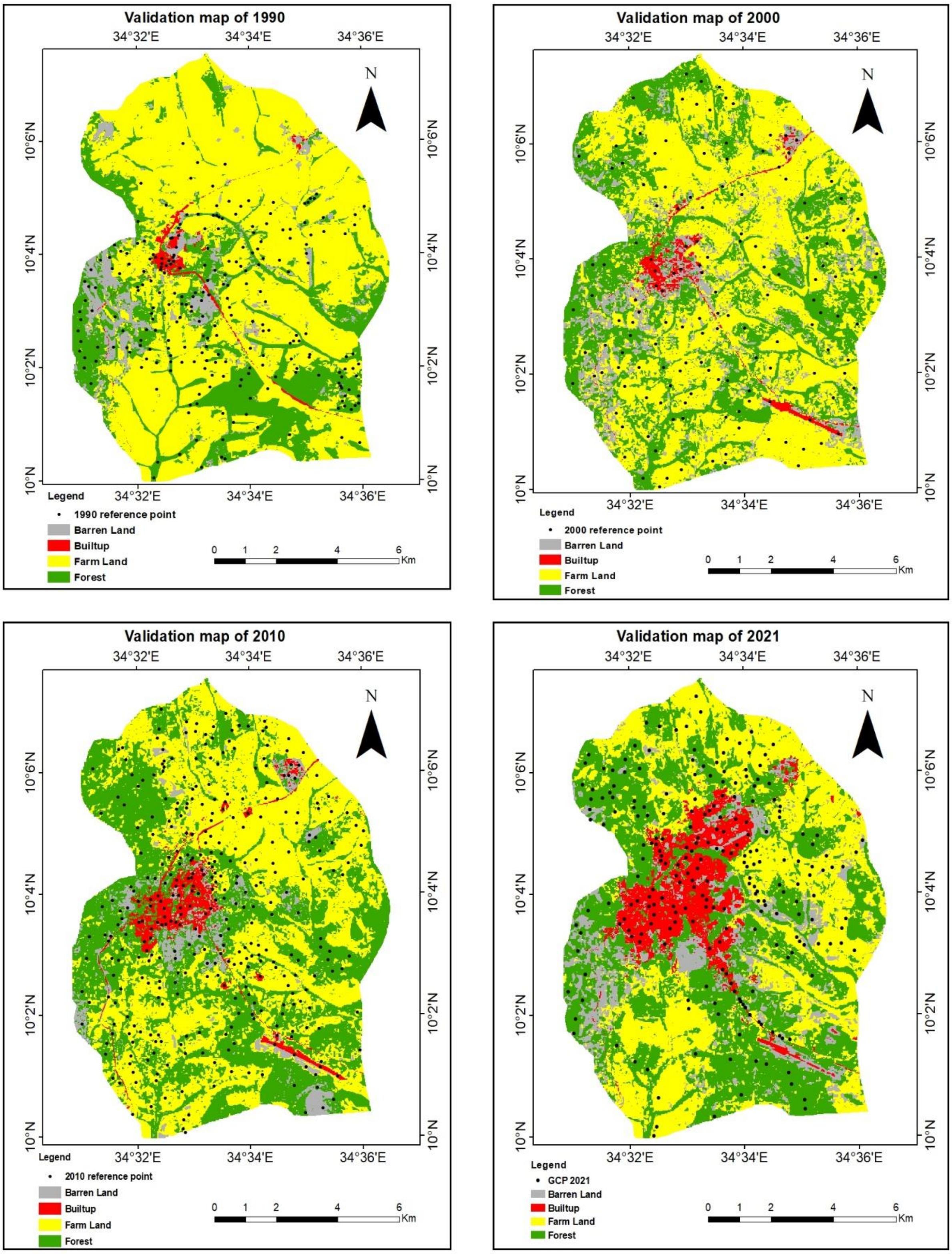

Appendix 3 sleuth model validation map

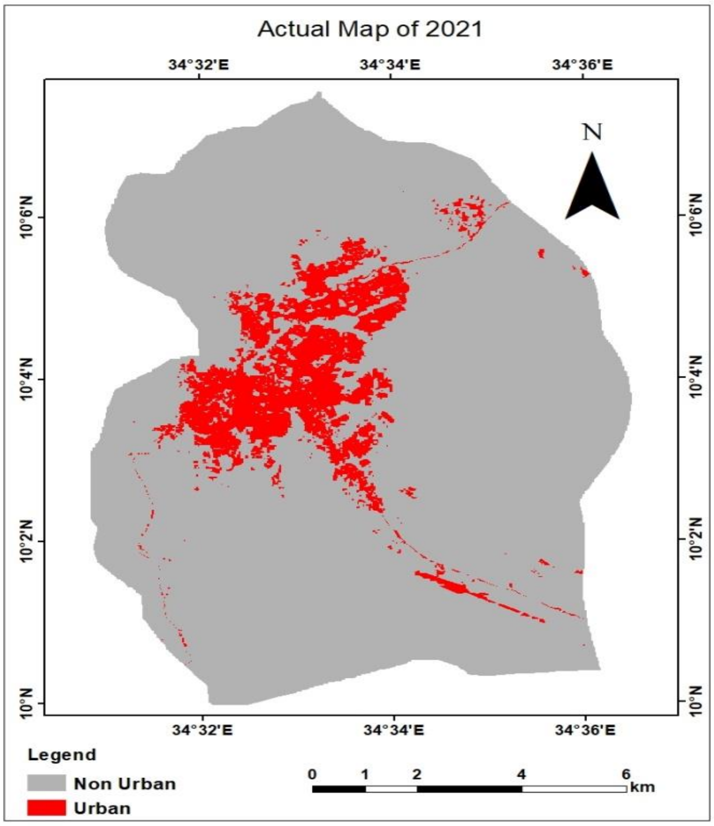

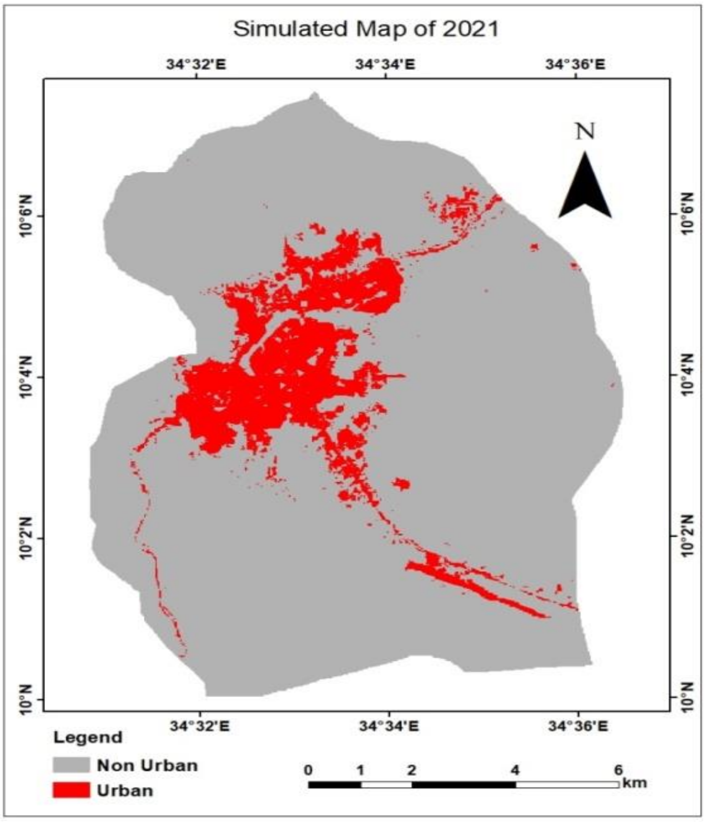

Appendix 4 SLEUTH Source code for simulation

```
# FILE: 'scenario file' for SLEUTH land cover transition model

#       (UGM  v3.0)

#       Comments start with #

# I.PATH NAME VARIABLES

INPUT_DIR=../Input/Assosa/

OUTPUT_DIR=../Output/Assosa_pre/

WHIRLGIF_BINARY=../Whirlgif/whirlgif

# II. RUNNING STATUS (ECHO)

ECHO(YES/NO)=yes

# III. Output Files

WRITE_COEFF_FILE(YES/NO)=yes

WRITE_AVG_FILE(YES/NO)=yes

WRITE_STD_DEV_FILE(YES/NO)=no

WRITE_MEMORY_MAP(YES/NO)=YES

LOGGING(YES/NO)=YES

# IV. Log File Preferences

LOG_LANDCLASS_SUMMARY(YES/NO)=yes

LOG_SLOPE_WEIGHTS(YES/NO)=no

LOG_READS(YES/NO)=no

LOG_WRITES(YES/NO)=no

LOG_COLORTABLES(YES/NO)=no

LOG_PROCESSING_STATUS(0:off/1:low verbosity/2:high verbosity)=1

LOG_TRANSITION_MATRIX(YES/NO)=yes
```

LOG_URBANIZATION_ATTEMPTS(YES/NO)=yes

LOG_INITIAL_COEFFICIENTS(YES/NO)=no

LOG_BASE_STATISTICS(YES/NO)=yes

LOG_DEBUG(YES/NO)= no

LOG_TIMINGS(0:off/1:low verbosity/2:high verbosity)=1

V. WORKING GRIDS

NUM_WORKING_GRIDS=5

VI. RANDOM NUMBER SEED

RANDOM_SEED=1

VII. MONTE CARLO ITERATIONS

MONTE_CARLO_ITERATIONS=10

VIII. COEFFICIENTS

CALIBRATION_DIFFUSION_START= 1

CALIBRATION_DIFFUSION_STEP= 1

CALIBRATION_DIFFUSION_STOP= 1

CALIBRATION_BREED_START= 23

CALIBRATION_BREED_STEP= 1

CALIBRATION_BREED_STOP= 23

CALIBRATION_SPREAD_START= 50

CALIBRATION_SPREAD_STEP= 1

CALIBRATION_SPREAD_STOP= 50

CALIBRATION_SLOPE_START= 22

CALIBRATION_SLOPE_STEP= 1

CALIBRATION_SLOPE_STOP= 22

```
CALIBRATION_ROAD_START=     13

CALIBRATION_ROAD_STEP=      1

CALIBRATION_ROAD_STOP=      13

PREDICTION_DIFFUSION_BEST_FIT=  2

PREDICTION_BREED_BEST_FIT=  67

PREDICTION_SPREAD_BEST_FIT=  31

PREDICTION_SLOPE_BEST_FIT=  9

PREDICTION_ROAD_BEST_FIT=  14

# IX. PREDICTION DATE RANGE

PREDICTION_START_DATE=2021

PREDICTION_STOP_DATE=2050

# X. INPUT IMAGES

#  format:  <location>.urban.<date>.[<user info>].gif

URBAN_DATA= assosa.urban.1990.gif

URBAN_DATA= assosa.urban.2000.gif

URBAN_DATA= assosa.urban.2010.gif

URBAN_DATA= assosa.urban.2021.gif

# Road data GIFs

#  format:  <location>.roads.<date>.[<user info>].gif

ROAD_DATA= assosa.roads.1990.gif

ROAD_DATA= assosa.roads.2000.gif

ROAD_DATA= assosa.roads.2010.gif

ROAD_DATA= assosa.roads.2021.gif

# Landuse data GIFs
```

```
#  format:  <location>.landuse.<date>.[<user info>].gif

LANDUSE_DATA= assosa.landuse.1990.gif

LANDUSE_DATA= assosa.landuse.200.gif

LANDUSE_DATA= assosa.landuse.2010.gif

LANDUSE_DATA= assosa.landuse.2021.gif

# Excluded data GIF

#  format:  <location>.excluded.[<user info>].gif

EXCLUDED_DATA= assosa.excluded.gif

# Slope data GIF

#  format:  <location>.slope.[<user info>].gif

SLOPE_DATA= assosa.slope.gif

# Background data GIF

#  format:   <location>.hillshade.[<user info>].gif

#BACKGROUND_DATA= demo200.hillshade.gif

BACKGROUND_DATA= assosa.hillshade.gif

# XI. OUTPUT IMAGES

WRITE_COLOR_KEY_IMAGES(YES/NO)=no

ECHO_IMAGE_FILES(YES/NO)=no

ANIMATION(YES/NO)= no

# XII. COLORTABLE SETTINGS

#  A. DATE COLOR SETTING

DATE_COLOR=     0XFFFFFF #white

#     3. PROBABILITY COLORTABLE FOR URBAN GROWTH

PROBABILITY_COLOR=   0,    1,          , #transparent
```

```
PROBABILITY_COLOR=   1,    10, 0X00ff33, #green
PROBABILITY_COLOR=   10,   20, 0X00cc33, #
PROBABILITY_COLOR=   20,   30, 0X009933, #
PROBABILITY_COLOR=   30,   40, 0X006666, #blue
PROBABILITY_COLOR=   40,   50, 0X003366, #
PROBABILITY_COLOR=   50,   60, 0X000066, #
PROBABILITY_COLOR=   60,   70, 0XFF6A6A, #lt orange
PROBABILITY_COLOR=   70,   80, 0Xff7F00, #dark orange
PROBABILITY_COLOR=   80,   90, 0Xff3E96, #violetred
PROBABILITY_COLOR=   90,  100, 0Xff0033, #dark red
#  C. LAND COVER COLORTABLE
#          pix, name,     flag,   hex/rgb, #comment
LANDUSE_CLASS=  0,  Unclass , UNC   , 0X000000
LANDUSE_CLASS=  1,  Urban   , URB   , 0X8b2323 #dark red
LANDUSE_CLASS=  2,  Agric   ,       , 0Xffec8b #pale yellow
LANDUSE_CLASS= 3,  Range   ,       , 0Xee9a49 #tan
LANDUSE_CLASS=  4,  Forest  ,       , 0X006400
LANDUSE_CLASS=  5,  Water   , EXC   , 0X104e8b
LANDUSE_CLASS= 6,  Wetland ,       , 0X483d8b
LANDUSE_CLASS=  7,  Barren  ,       , 0Xeec591
#  D. GROWTH TYPE IMAGE OUTPUT CONTROL AND COLORTABLE
VIEW_GROWTH_TYPES(YES/NO)=NO
GROWTH_TYPE_PRINT_WINDOW=0,0,0,0,1990,2050
PHASE0G_GROWTH_COLOR=  0xff0000 # seed urban area
```

PHASE1G_GROWTH_COLOR= 0X00ff00 # diffusion growth

PHASE2G_GROWTH_COLOR= 0X0000ff # NOT USED

PHASE3G_GROWTH_COLOR= 0Xffff00 # breed growth

PHASE4G_GROWTH_COLOR= 0Xffffff # spread growth

PHASE5G_GROWTH_COLOR= 0X00ffff # road influenced growth

E. DELTATRON AGING SECTION

VIEW_DELTATRON_AGING(YES/NO)=NO

DELTATRON_PRINT_WINDOW=0,0,0,0,1990,2050

DELTATRON_COLOR= 0x000000 # index 0 No or dead deltatron

DELTATRON_COLOR= 0X00FF00 # index 1 age = 1 year

DELTATRON_COLOR= 0X00D200 # index 2 age = 2 year

DELTATRON_COLOR= 0X00AA00 # index 3 age = 3 year

DELTATRON_COLOR= 0X008200 # index 4 age = 4 year

DELTATRON_COLOR= 0X005A00 # index 5 age = 5 year

XIII. SELF-MODIFICATION PARAMETERS

ROAD_GRAV_SENSITIVITY=0.01

SLOPE_SENSITIVITY=0.1

CRITICAL_LOW=0.97

CRITICAL_HIGH=1.3

#CRITICAL_LOW=0.0

#CRITICAL_HIGH=10000000000000.0

CRITICAL_SLOPE=15.0

BOOM=1.01

BUST=0.09

Appendix 5 First five rows of the control_stats.log file after the coarse calibration mode run sorted in descending order by the Lee Sallee metric.

Run	Product	Compare	Pop	Edges	Cluster	s Size	Leesale	e Slope
220	0	0.7	0.7	0.6	1	0.2	0.0981	0.8
221	0	0.7	0.7	0.6	1	0.2	0.0981	0.8
305	0	0.8	0.7	0.7	0.7	0.2	0.09786	0.8
306	0	0.8	0.7	0.7	0.7	0.2	0.09786	0.8
440	0	0.7	0.7	0.6	0.1	0.3	0.09763	0.8

%Urban	Xmean	Ymean	Rad	Fmatch	Diff	Brd	Sprd	Slp	RG
0.7	0.9	0.3	0.6	0.6	1	25	75	100	1
0.7	0.9	0.3	0.6	0.6	1	25	75	100	25
0.7	0.9	0.9	0.6	0.6	1	50	50	25	1
0.7	0.9	0.9	0.6	0.6	1	50	50	25	25
0.7	1	0.4	0.7	0.6	1	75	50	75	1